PROCEEDINGS OF THE ROYAL SOCIETY A

rspa.royalsocietypublishing.org

Research

Article submitted to journal

Subject Areas:
xxxxx, xxxxx, xxxx

Keywords:
xxxx, xxxx, xxxx

Author for correspondence:
Manoj Srinivasan
e-mail: srinivasan.88@osu.edu

Walking on a moving surface: Energy-optimal walking motions on a shaky bridge and a shaking treadmill reduce can energy costs below normal

Varun Joshi and Manoj Srinivasan

Mechanical and Aerospace Engineering, The Ohio State University, Columbus, OH 43201 USA

Understanding how humans walk on a surface that can move might provide insights into, for instance, whether walking humans prioritize energy use or stability. Here, motivated by the famous human-driven oscillations observed in the London Millennium Bridge, we introduce a minimal mathematical model of a biped, walking on a platform (bridge or treadmill) capable of lateral movement. This biped model consists of a point-mass upper body with legs that can exert force and perform mechanical work on the upper body. Using numerical optimisation, we obtain energy-optimal walking motions for this biped, deriving the periodic body and platform motions that minimize a simple metabolic energy cost. When the platform has an externally-imposed sinusoidal displacement of appropriate frequency and amplitude, we predict that body motion entrained to platform motion consumes less energy than walking on a fixed surface. When the platform has finite inertia, a mass-spring-damper with similar parameters to the Millennium Bridge, we show that the optimal biped walking motion sustains a large lateral platform oscillation when sufficiently many people walk on the bridge. Here, the biped model reduces walking metabolic cost by storing and recovering energy from the platform, demonstrating energy benefits for two features observed for walking on the Millennium Bridge: crowd synchrony and large lateral oscillations.

Royal Society Publishing
Informing the science of the future

1. Introduction

While many modern humans mostly walk on stable fixed surfaces such as tiled floors, concrete pavements, and solid ground, humans can walk and run on a wide variety of surfaces with different compliances, damping, and granularity, and do so with remarkable stereotypicality (e.g., [1,2]). In a famous public event, when pedestrians were allowed on to the shaky walking surface of the London millennium bridge [3,4], many walked in synchrony with each other and the bridge, with larger-than-normal step widths and therefore applied larger-than-normal sideways forces on the bridge. This eventually resulted in large lateral oscillations of the bridge, causing more and more people to walk the same way. Similar lateral oscillations have been observed in other footbridges as well [5–7]. Experiments with humans walking on laterally oscillating treadmills have shown a similar response, namely larger sideways forces and wider step widths [8]. In this article, we examine the mechanics of walking on a shaky bridge and walking on an externally shaken treadmill by deriving the energy optimal motions of a simple mechanics-based mathematical model of a biped, and showing, perhaps surprisingly, that walking on such shaky surfaces can reduce walking energy requirements at high oscillation amplitudes.

A natural hypothesis is that humans change their walking gait on a shaky bridge to be more stable i.e., not fall down. Wider step-widths might improve sideways stability [9] and humans use sideways foot-placement to avoid falling sideways and recover from sideways perturbations [10,11]. Indeed, a few authors [7,8] have used 'inverted pendulum models' of lateral pedestrian motion with step-width-control-based stabilization to explain pedestrian-driven bridge oscillations. In these models, even though the pedestrians cannot influence the motion of the bridge (the bridge is assumed to oscillate sinusoidally with fixed amplitude and frequency), they perform mechanical work on the bridge; thus, the modeled pedestrian was found to act, effectively, as a negative damper on bridge motion, producing an additional sideways force at the bridge vibration frequency. In contrast to this stabilization hypothesis, Strogatz et al. [4] modeled the pedestrians as abstract phase oscillators with randomly distributed oscillation frequencies (close to the bridge's natural frequency), coupled to the same mass-spring-damper modeling the London Millennium Bridge. Here, as the pedestrian count increased beyond a critical number, they synchronized with each other and the bridge, leading to a steady-state motion with large bridge oscillation amplitude. While these models provide insight into the causes for additional sideways forces and synchronization, none of these models have considered the fully-coupled interaction of one or more humans with the bridge during forward walking.

In this article, we take an alternative approach to modeling the human response to surface motion. One of the most successful predictive theories of steady-state human locomotion is that humans move in a manner that minimizes the metabolic cost of walking. Experimental studies have shown that humans use the metabolically optimal speed, step length, step width, arm swing, gait transition speeds [12–16], etc. Energy-optimal motions in computational models of a biped have explained numerous features of human locomotion [17–25]. Remarkably, even with little practice, humans seem to find energy optimal movement patterns even for novel tasks such as sideways walking [26], split-belt treadmill walking [27], and tasks with unusual frequency and step length constraints [28]. Therefore, we consider the hypothesis that humans move on shaky bridges and shaking treadmills in a manner that minimizes the metabolic energy cost of walking.

Here, we predict walking motions by numerical optimisation, deriving the periodic motions that minimizes a work-based metabolic cost of walking; we consider the modeling analogues of both walking on a shaky bridge and walking on an externally shaken treadmill, considering a range of speed and other parameter values. Our biped model, introduced in section 2, is capable of arbitrarily complex walking motions [21,23], allowing for a wide range of pedestrian and bridge motions. We assume that the pedestrians walk in synchrony with the platform on which they walk and show that in some model parameter regimes, entrained walking on a shaken treadmill or a shaky bridge can have lower energy costs than normal walking on a non-moving surface. We examine the effect of the number of pedestrians, the bridge stiffness and the damping on the

amplitude and frequency of oscillations, and suggest that metabolic energy minimization could be an alternative explanation of the unusual interaction between humans and the walking surface.

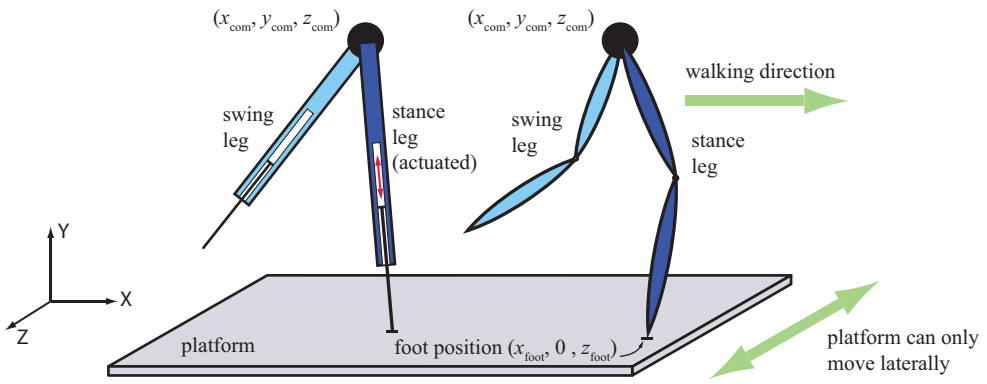

Figure 1. Biped model on a platform. The biped has a point-mass upper body and can move in all three directions: forward (X-direction), vertically (Y-direction) and laterally (Z-direction). The platform can only move laterally. Two possible embodiments of the leg are shown, one with a knee and one with a telescoping actuator.

2. A 3D biped model for walking on a moving surface

We consider a simple biped consisting of a point mass upper body of mass m and two legs, as shown in figure 1, capable of three-dimensional movement. During each step, only one leg is in contact with the ground while the other one can be swung arbitrarily. The legs are massless for dynamical purposes, so that leg swing does not affect the upper body, but have a mass m_{foot} to calculate the leg-swing-cost (as in [23,29]; see appendix A2). Both legs have point feet and their hip joints are coincident with the point-mass upper body, so that the model has zero hip-width. When a leg is in contact with the ground (that is, in 'stance phase'), the stance-leg-knee can flex and extend, applying arbitrarily varying forces on the upper body, thereby changing the effective leg length. These motions are subject to a maximum leg-length and leg-force constraint. It is further assumed that the foot does not slip relative to the walking surface during stance. Flight (when neither leg contacts the ground) and double-support or double-stance (when both legs are contact the ground) are not considered [21,29], as their absence seems optimal for this class of biped models at walking speeds [23]. Figure 1 shows two possible embodiments of the leg, one with a knee, one with a telescoping actuator [21]; the knee is just one way of accomplishing leg length changes. The model's motion capability is independent of the embodiment [23].

In its leg force capability, the biped model is a generalization of the classic inverted pendulum walking model [21,30,31] and various spring mass models [32,33]. A planar version of this biped has been shown to discover both walking and running like gaits when moving in a straight line while minimizing energy cost per unit distance [23]. Here, in addition to allowing three-dimensional movement for the center-of-mass, we allow the walking surface to move laterally, i.e., perpendicular to walking direction (figure 1).

We consider two types of walking surfaces or "platforms":

- **Infinite inertia platform**, for which the platform can affect biped movement, but the biped cannot affect platform movement. The platform movement is externally specified, as in the case of a treadmill oscillated sideways e.g., sinusoidally. Thus, we will also refer to this as the "shaken treadmill" case.

- **Finite inertia platform**, a one-degree-of-freedom mass-spring-damper system, whose motion can be influenced by the biped's leg forces, as in equation A1.5. We only consider a lateral degree-of-freedom. Examples include light footbridges and walkways. Thus, we will also refer to this as the "shaky bridge" case.

The differential equations of motion describing the motion of the biped model and the platform are given in appendix A1, equations A1.2-A1.4 for the biped and equations A1.5-A1.6 for the two types of platforms.

The metabolic energy cost function is a sum of four components [23], described with equations in appendix A2: 1) The resting metabolic rate, a constant cost per unit time, 2) Stance-work cost, proportional to a linear combination of the positive and negative work of the legs during stance, 3) Stance force cost, proportional to integrated leg force during stance, 4) Swing leg cost, proportional to the work needed to move the swing leg to its next stance position.

We seek the walking motions, periodic over two walking steps (equal to one stride), that minimize the metabolic cost of forward progression. Thus, for either platform model, we parameterize the space of possible walking motions using finitely many unknowns, using initial conditions for the steps and describing the leg forces $F(t)$ using piecewise linear functions [21]. We use numerical optimisation to determine the values of these unknown parameters so as to produce net forward movement while minimizing an energy cost function, subject to leg length, leg force, and periodicity constraints. See appendix A3 for computational details (also [21,23]). For some calculations, we specify the speed and stride length – and consequently the stride frequency – whereas in other calculations, all such quantities are unknowns to be determined by the optimisation. We specify speed and stride length when we wish to isolate the effect of stance work and force costs, as all other cost terms are constant – independent of body motion – for a given speed and stride length.

For reference, we note that for this biped model, it has been shown [21,23] that the planar "inverted pendulum walking" motion minimized this metabolic cost in the absence of any surface motion. In this optimal walking motion, each stance phase consists of an inverted pendulum-like motion of the body vaulting over a straight leg and the step-to-step transition accomplished using a push-off impulse by the trailing leg, followed by a heel-strike impulse by the leading leg. The stance work cost is entirely due to the positive and negative work performed during the push-off and heel-strike impulses. Of course, when the walking surface is moving, this planar walking motion will no longer be feasible.

Note that when the platform is moving, we do assume that the human walking motion is entrained to the platform's motion so that the state of the whole system is periodic. For the infinite inertia platform, our basic calculation assumes equality of the stride period and platform period. For the finite inertia platform, our assumption does allow the bridge to perform multiple periods per human stride, but such motions were never optimal. Optimisation calculations with periodicity of multiple human steps are more computationally expensive and were not considered. Further, we did not consider optimisations in which the system can be non-periodic; as described in the discussion, such non-periodic optimisation calculations are conceptually problematic or also computationally expensive.

In the following sections, all results are presented in terms of non-dimensional quantities, obtained by normalization using appropriate combinations of the mass of the body, the length of the fully extended leg, and the acceleration due to gravity; the exact normalizations for non-dimensionalization are described in appendix A1.

3. Infinite inertia platform: walking on oscillating treadmills

In this calculation, we couple the biped to an infinite inertia platform, sinusoidally oscillating sideways (equation A1.6). As noted, this is a model of a person walking on an externally oscillated treadmill, with the person having no ability to affect the treadmill's motion. We consider a range of platform oscillation amplitudes and frequencies. The walking stride frequency is assumed to

match the platform oscillation frequency, so that the biped is entrained to the platform, i.e. during one walking stride, exactly one platform oscillation occurs. The initial position and velocity of the body center of mass, the relative phase between the platform motion and the gait cycle, the position of the foot during the second step and the piecewise-linear forces exerted by leg on the center of mass are parameters of the optimisation. The position of the foot during the first step is taken as the origin for the coordinate system.

For a fixed non-dimensional walking speed of 0.4 (about 1.2 m/s for a person with leg length 0.95 m), we determine the optimal walking motion for a range of platform amplitudes and frequencies. The range of frequencies was chosen to be around the optimal non-dimensional stride frequency (around 0.4) for the biped while walking without any platform oscillation (planar walking). Figure 2a shows that the biped can reduce its metabolic cost of walking by appropriately coordinating the leg forces, the initial position and velocity of the center of mass and the phase relative to the platform motion. In particular, we find that even for a non-dimensional oscillation amplitude of 0.03 (about 3 cm), there is a noticeable reduction in the model metabolic cost for a frequency beyond a non-dimensional frequency of 0.3. Within the frequency range explored here, higher platform oscillation amplitudes allow greater cost reduction for a broader range of frequencies. Figure S8 of Supplementary Appendix shows that the qualitative phenomenon of energy cost reduction persists for a range of forward speeds and model parameters.

Figures 2b-c show the body trajectory for a particular platform oscillation amplitude and frequency, indicating that the lateral body motion is smaller than the platform motion. Analogous to walking on a non-moving surface [21,23], we find that the optimal motion in the presence of platform motion is also an inverted pendulum-like motion with impulses corresponding to heel-strike and push-off – this is a non-planar inverted pendulum walking motion. Figures 2b-c show such an inverted pendulum like motion of the center of mass; figure S1a of the *Supplementary Appendix*, obtained by allowing arbitrary piecewise linear leg force changes, shows that the optimal motion displays the following features of inverted pendulum walking.. The leg is always stretched close to the maximum limit, i.e. the biped walks with a straight knee during stance, with a large step width so as to manage the lateral platform movement. The push-off and heel-strike occur as brief impulses near the extremes of platform motion (as in [21]), enabling the instantaneous velocity change from one pendular step to the next; the push-off does positive work and the heel-strike does negative work. This optimal motion corresponds to a relative phase of about $\pi/2$ between the platform motion and the biped motion. When the platform moves leftward, the body remains to the left of the foot. As the body moves forward during a given stance phase, the foot (fixed relative to platform) moves inward toward the body from heel-strike to push-off.

For some oscillation parameters, we found that it is possible for the model to walk on an oscillating platform without any heel-strike or push-off impulses — in other words, smoothly transitioning from one inverted pendulum stance phase to the next. Such a motion would optimize the "stance work cost" portion of our metabolic cost model, making this leg work equal zero; see *Supplementary Appendix*, figure S1b. But such a motion is not optimal for the full metabolic cost (i.e., not one of those found in Figure 2a), because other components of metabolic cost (leg swing and stance force costs) are higher for this motion.

We find that the mechanism by which the oscillating platform reduces the cost of walking is by reducing the necessary push-off and heel-strike impulse magnitudes, thereby reducing the positive and negative stance leg work during these impulses. The variation in energy cost components can be seen in figure S13 (*Supplementary Appendix*), which shows that the decrease in the stance work cost more than compensates for a slight increase in stance force cost. By appropriately synchronizing the body motion with the platform motion, one can let the platform perform some of the mechanical work on the body that would otherwise have to be done by the legs. The leg work performed by the impulses are smaller because a smaller velocity direction change is required across the step-to-step transition than in normal walking. In particular, the out of plane motion of the center of mass makes the sagittal-plane projection of the center of

mass trajectories much flatter than in normal walking – ultimately leading to the smaller velocity direction change across the step to step transition [34,35]. See *Supplementary Video* 1 for animations of these optimal walking motions.

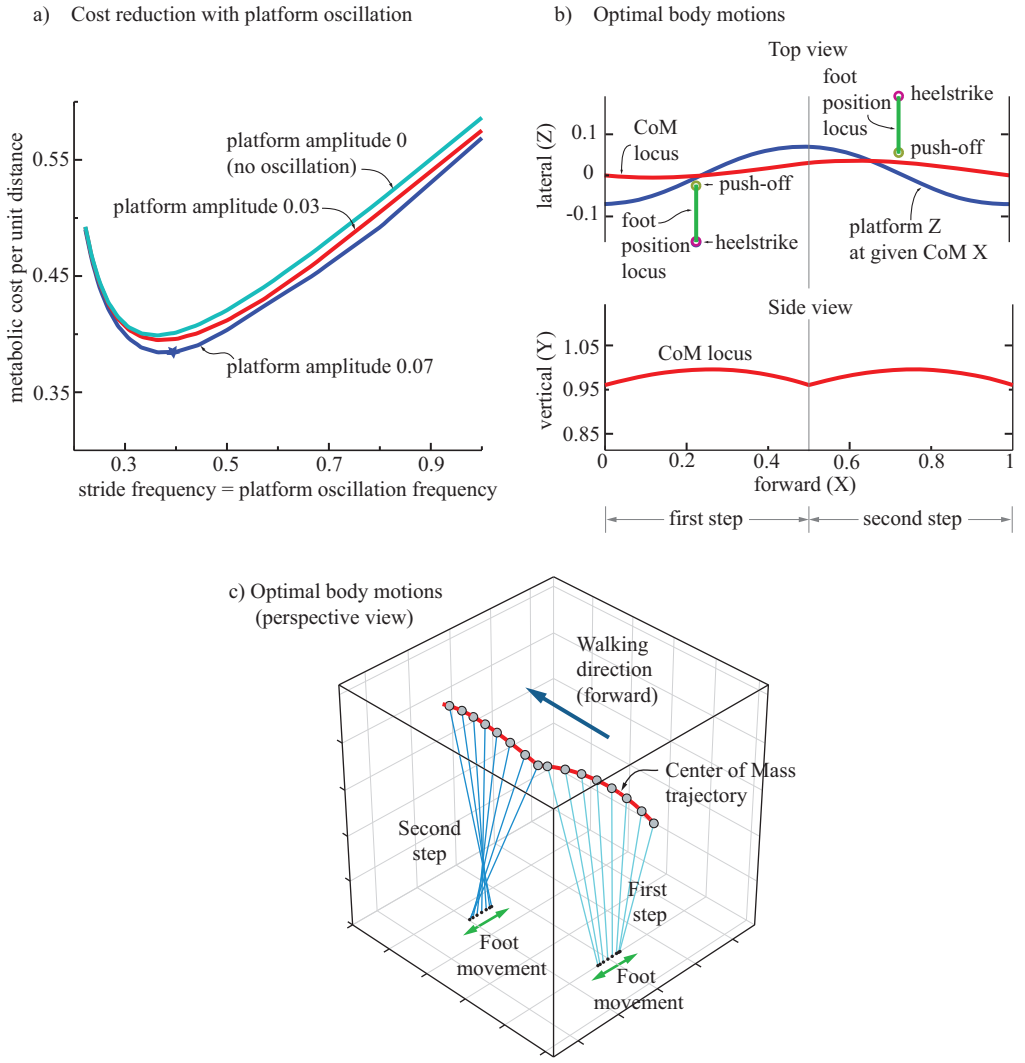

Figure 2. Energy-optimal walking on an oscillating infinite inertia platform. a) Energy cost per unit distance versus oscillation frequency for 0, 0.03 and 0.07 non-dimensional oscillation amplitudes. Walking speed is fixed at 1.2 m/s (non-dimensional speed = 0.4). Thus, we see that oscillating platforms reduce walking energy cost for a range of oscillation frequencies. b) Motion of the center of mass and platform for 0.07 non-dimensional platform amplitude and non-dimensional frequency 0.4, denoted by a 'star' ($\star$) in panel-a. The blue curve shows the corresponding position of the platform for each forward position of the center of mass, the red curve represents the motion of the center of mass, the green lines are the loci of the feet, with open circles showing the position of the foot at the heel-strike (red) and push-off (green). c) The 3D optimal body motions are shown in perspective view. The leg directions are shown as blue lines between the foot positions (filled black circles, moving sideways) and the center of mass positions (black circles with gray fill). The two steps are reflection symmetric about a mid-line as seen in panel-b, even though not immediately apparent in this 3D view.

4. Finite inertia platform: walking on shaky bridges

We consider a finite inertia platform that is a one degree-of-freedom spring-mass-damper system (as also in [4]). This model is a closer approximation to a bridge than an externally oscillated infinite inertia platform, because the pedestrian can actually influence the platform motion and this platform motion is not restricted to purely sinusoidal oscillations. Again, as for the infinite inertia case above, we first established that even when we allow arbitrary leg length changes and piecewise linear leg force changes, the optimal motion is a 3D non-planar inverted pendular motion with push-off and heel-strike impulses, as shown in figure S7 of the *Supplementary Appendix*. Therefore, the calculations described below assume the biped walks using exactly an inverted pendulum gait using the maximum leg-length. This inverted pendulum simplification speeds up the optimisations and improves convergence. Push-off impulses are parameters of the optimisation, but heel-strike impulses are computed based on the motion of the center-of-mass, assuming a plastic collision (as in [29]), to make the leg-length-rate after heel-strike exactly zero.

The stiffness, mass and damping of the platform are selected as equal to the corresponding modal quantities for the Millennium Bridge (as in [4]); see appendix A1 for these and other human parameters used. Further, to establish more general trends, we also consider multiples of these stiffness and damping values, denoted 0.5x, 2x, etc. The unknown parameters for optimisation are stride length, stride frequency, initial position and velocity of both the centre of mass and the platform, the position of the foot for the second step, and the magnitudes of push-off impulses; we do not constrain forward speed. Once again, the position of the foot during the first step is taken to be the origin of the co-ordinate system. The initial conditions of the platform serve the same purpose as the relative phase from the infinite-inertia calculation. Unlike the infinite-inertia platform, the platform oscillations are not constrained in any way here, in that there can be any number (even non-integer number) of oscillations per stride and the amplitude can be as large or as small as needed. This allows for solutions where there is no platform oscillation. For each stiffness and damping value, we perform the optimisation calculations for a range of pedestrian counts $N_{\text{pedestrians}}$ between 1 and 1000 or 1500. We model $N_{\text{pedestrians}}$ pedestrians simply as one large pedestrian with $N_{\text{pedestrians}}$ times the mass m of a single pedestrian, thus assuming that all $N_{\text{pedestrians}}$ pedestrians walk in synchrony with each other. For reference, at $N_{\text{pedestrians}} \approx 1600$, the total pedestrian mass equals the bridge mass.

First, for stiffness and damping equal to that of the Millennium Bridge (1x damping curves in Figure 3a,b), we find that a walking motion that substantially oscillates the platform is optimal when the pedestrian number increases beyond a critical level, about 750 pedestrians. The reduction in metabolic cost from the oscillating bridge is small. Nevertheless, these results show that if there are a large number of people walking in synchrony, they can potentially lower their metabolic cost by shaking the bridge. For lower numbers of pedestrians, the optimal walking motion is planar, without oscillating the bridge. Figure 4 shows the optimal body and foot motion for $N_{\text{pedestrians}} = 1000$ and the London Millennium Bridge parameters; see also figure S2a of *Supplementary Appendix* and *Supplementary Video* 2.

Figure 3a,b also shows these trends for a range of damping values from 0x to 1x the Millennium Bridge damping, keeping the stiffness fixed at that of the Millennium Bridge (1x stiffness). As damping is decreased from 1x, the critical number of pedestrians required to make the oscillating platform solution optimal reduces; for instance, at 0.4x damping, the critical number is about 250 pedestrians (Figure 3a,b). Independent of platform damping, increasing the number of pedestrians beyond the critical number leads to an increase in platform oscillation amplitude and a corresponding decrease in metabolic cost per unit distance; this decrease in metabolic cost is smaller for higher platform damping (Figure 3a,b). For the oscillating solutions, the pedestrian walks with a large step width, which increases with platform oscillation amplitude and number of pedestrians (figures S3-S5, *Supplementary Appendix*). We also note that these qualitative trends persist for a large range of model parameters (foot mass, resting rate, and stance force cost scaling) as shown in figure S9 of *Supplementary Appendix*.

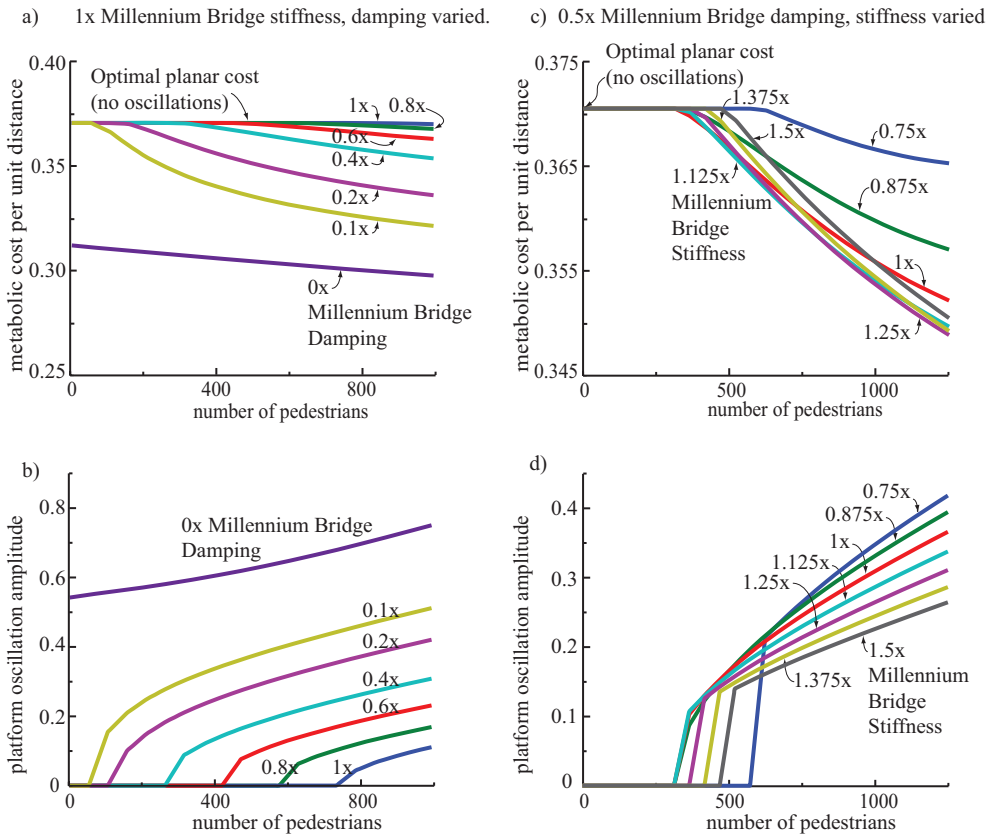

Figure 3. Energy-optimal walking on the finite inertia platform shows platform oscillations reduced metabolic cost when there are sufficiently many pedestrians. a) Metabolic energy per unit distance versus number of pedestrians for the exact Millennium Bridge stiffness and for different multiples of the Millennium Bridge damping. Lower damping and more pedestrians allow for greater reduction in the energy cost. b) Platform oscillation amplitude versus number of pedestrians for damping in multiples of the Millennium Bridge damping and the exact Millennium Bridge stiffness. More pedestrians and lower damping lead to higher oscillation amplitudes. c) Metabolic energy per unit distance versus number of pedestrians for stiffness in multiples of the Millennium Bridge stiffness and the 0.5x the Millennium Bridge damping. Higher stiffness and more pedestrians allow for greater reduction in the energy cost. d) Platform oscillation amplitude per unit distance versus number of pedestrians for stiffness in multiples of the Millennium Bridge stiffness and the 0.5x the Millennium Bridge damping. Lower stiffness and more pedestrians allow for greater oscillation amplitudes. See *Supplementary Appendix*, figures S3 and S5, for additional details such as optimal step widths, speed, and stride frequency.

Fixing the damping to 0.5 times that of the Millennium Bridge and varying the platform stiffness, we see similar qualitative behaviour: for all stiffnesses, beyond a critical number of pedestrians, a larger number of pedestrians leads to oscillating platforms with a corresponding reduction in metabolic cost per unit distance. In Figure 3c,d, for the number of pedestrians explored, we see that the metabolic energy cost per unit distance reduces with increasing stiffness from 0.75x to 1.25?; the metabolic cost increases with increasing stiffness from 1.25x to 1.5?. The critical number of people shows the opposite trend with changing stiffness. Higher stiffness lead to lower oscillation amplitudes. Overall, while the trends respond in a simple monotonic manner to changes in platform damping, they respond non-monotonically to changes in platform stiffness.

The principal mechanism for the metabolic cost reduction is the lowering of the stance work required of the legs, reflected in smaller magnitudes for the heel-strike impulse. The effect of oscillations on the individual components of the cost function can be seen in figures S10 and S11 of the *Supplementary Appendix*. The reduction in the required leg work is greatest when damping is zero, when an oscillating platform solution is optimal for even one pedestrian (see figure S4 for results for the zero damping case). When there is finite damping, the positive work at push-off should sufficiently exceed the negative work at heel-strike so as to compensate for the energy lost to the bridge's structural damping. Again, the sideways motion of the body and the bridge reduces the necessary change in body velocity direction at the step-to-step transition, thereby decreasing the work required of the push-off and heel-strike impulses [34,35].

Why is there a critical pedestrian number for oscillating solutions to be better than planar solutions? The reason appears to be the presence of damping. In general, we find that increasing the number of pedestrians lowers the metabolic energy cost per unit distance in the oscillating platform solution. As noted, when there is considerable damping, net positive leg work needs to be performed to replace the energy lost in the bridge motion. This additional net positive work requirement (for a given platform amplitude) is distributed over all pedestrians, and consequently, for a large enough pedestrian count the oscillating solution becomes better than the planar solution.

The non-dimensional optimal speeds for the range of parameters considered appear to be between 0.3 and 0.45, which correspond to 0.95 and 1.4 m/s. The model parameters corresponds to a slower-than-natural optimal speed for planar walking on a non-moving platform, but this optimal speed can be made to agree with normal human optimal speeds by choosing an appropriate resting metabolic rate, without changing any of the qualitative phenomena of energy cost reduction by a sideways shaking bridge..

For any given speed, the oscillating solution has lower cost than the planar solution only when the non-dimensional stride frequency is around 0.3 as demonstrated in figure S12 of the *Supplementary Appendix*, which was obtained by solving the optimisations for a range of fixed walking speeds and stride lengths for 1000 pedestrians. This optimal stride frequency is also close to the bridge's natural frequency (≈ 0.33).

5. Discussion

The simple biped model suggests that walking on a laterally oscillating platform could be more efficient than planar walking in terms of metabolic energy cost. For walking on the finite inertia platform (shaky bridge), we find that the optimal solution is inverted pendulum walking with stride frequency entrained to the platform oscillation frequency, with near 0 phase difference between the pedestrian and the platform. These results for the model are similar to observations made about humans walking on the London Millennium Bridge [3] as well as on laterally oscillating treadmills [36]. However, on the infinite inertia platform, the optimal for our model was closer to $\frac{\pi}{2}$ phase difference.

While we have shown that the bipeds can potentially reduce the energy cost by synchronising their walking with the platform's motion, we have not ruled out the possibility of some arbitrarily complex non-periodic motion of the system that has an even lower energy cost. We did not do optimisations allowing non-periodic motions for two complementary reasons – the same implicit reasons why almost every biped walking optimisation has assumed periodicity. First, allowing the initial state to be different from the final state allows efficient forward movements that we would not call walking: for instance, turning off all the muscles and falling forward; or entirely using up some initially stored energy in the bridge to move forward, but only for a couple of steps. Such non-locomotor behaviors might be ruled by requiring persistent walking for sufficient distance, but then the resulting optimisation over a large number of steps would be vastly more computationally intensive. We hope to consider optimisations with multiple independent pedestrians or with periodicity over multiple strides in future work.

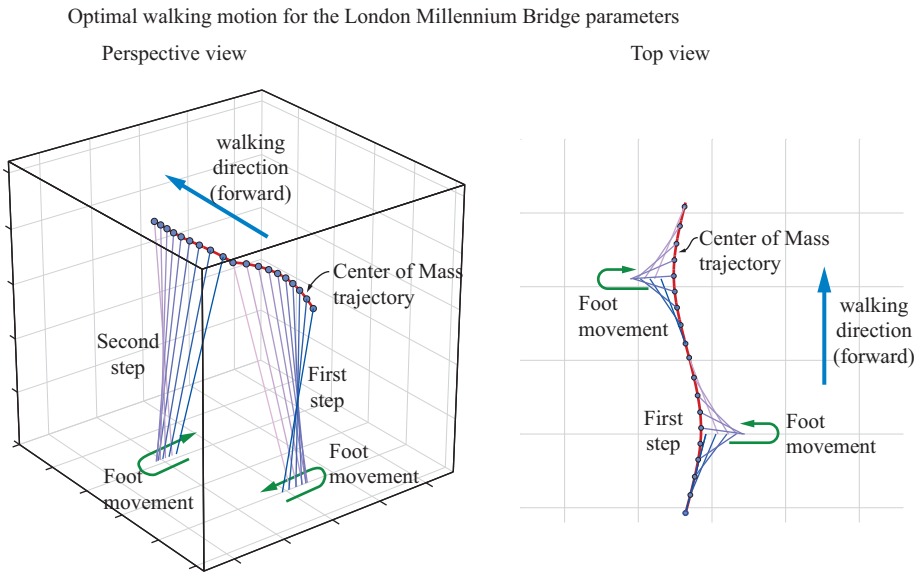

Figure 4. Optimal walking motions for London Millennium Bridge parameters. Perspective view and top view (orthogonal projection) of the center of mass trajectory for $N_{\text{pedestrians}} \approx 1000$, non-dimensional walking speed is close to 0.3 and non-dimensional stride-frequency is about 0.29. Leg directions are shown between corresponding foot and center of mass positions. The foot moves outward and then inward in a single step, as the body moves forward. See *Supplementary Appendix* figure S2 for another representation of the same information and *Supplementary Video* 2 for an animation of this motion.

For the models considered here, planar walking movement and zero step-width is optimal when the platform is not moving. However, humans walk with non-zero step width even in normal gait, perhaps because of having finite hip-widths [15]. Thus, normal human walking exerts a small sideways force even in the absence of platform oscillation. To understand the qualitative effects of having a minimum step width, we repeated the optimisation calculations with the finite inertia platform while constraining the walking step width to be at least the normal human step width (about 0.15 leg lengths), so that even normal walking produced sideways leg forces for the model. Even with this non-zero step width constraint, one could have non-oscillating solutions if one half of the pedestrians were exactly out of sync with the other half, or if all pedestrians had random phase relative to each other. Such non-oscillating solutions were sub-optimal. This step-width constraint leads to solutions with oscillating platforms and synchronized pedestrians for all pedestrian counts (see *Supplementary Appendix*, figure S6). For higher pedestrian numbers, the optimal solutions are identical to those obtained without the step width constraint and for lower pedestrian numbers, the optimal solution simply uses the minimum step width allowed (instead of zero, figure S6). The finite step-width solutions have higher cost than the zero step-width solution with no oscillations, but as before, the cost decreases as the number of pedestrians increases (figure S6).

Optimizing metabolic energy cost for this simple model can reproduce some aspects of human behaviour, however, given the simplicity of the model compared to a human, it may only predict qualitative aspects of phenomena while having quantitative differences with experiments. For example, the optimal solution discovered by this model for the exact parameters of the London Millennium Bridge needs a large number of pedestrians, about 750, for the onset of large bridge oscillations whereas published results are closer to 160. The use of periodicity constraints further prevents us from looking at the transient motion before the onset of steady state.

We assumed that human walkers will entrain to platform frequency, partly based on the observed steady-state motion of pedestrians on the London Millennium Bridge [3]. For the infinite inertia platform, the assumption that entrainment always occurs at steady state is likely reasonable for lateral oscillations near human stride frequencies, but may not hold true for oscillations much faster or slower than the stride frequencies, as found in [37] (see also [38] for entrainment studies with periodic torque perturbations to ankle, instead of surface oscillations). Without the assumption of entrainment, the energy optimisation calculation must be over all non-periodic walking strategies, which makes the optimisation intractable.

Our predictions that metabolic cost can be reduced by lateral motion can be directly tested in two kinds of experiments, analogous to the infinite and finite inertia cases we considered: (1) experiments with externally laterally oscillated treadmills with associated metabolic measurements [8,37], ensuring that the oscillations do not happen too slowly (as in [37]); (2) experiments in which the lateral degree of freedom is a simple spring-mass-damper, which can be simulated, for example, by placing a sufficiently light treadmill on wheels facing sideways and connecting the treadmill to the wall using springs, bungee cords, or elastic straps. In both these types of experiments, it would be of interest to test both the immediate dynamic and metabolic response of the human subject (within seconds and minutes), as well as the response after sufficient training (for a few hours, say). Energetics as the primary explanation for the Millennium Bridge phenomenon can be credible only if the humans entrain to optimal walking motions on the time-scale of less than a minute; there is some evidence for such fast optimisation time-scales in human locomotion [26,28,39,40]. The experiments described above could also measure the forces exerted by the legs on the ground and the work performed by the legs; our models predict that the impact forces (force peaks in walking) will be reduced if there is appropriate entrainment to sideways movement. If impact forces are indeed reduced in experiment, one could use such laterally oscillated treadmills for low-impact workouts. We could use models and methods similar to those used here to study locomotion on other types of compliant surfaces, for instance, non-human primate locomotion on flexible tree branches [41,42] or humans running [1,43].

We have shown the theoretical possibility of metabolic cost reduction only when a large number of people act in synchrony to shake a bridge (at least for some bridge parameters). This result could be considered similar to the posited reduction in locomotor metabolic cost in other contexts such as bird flying in formation [44] and fish swimming in a school [45], although in these other contexts, the different individuals may benefit by different amounts unlike in our model.

We have focused on energy optimality as a theory for human walking strategies while on a moving surface. One complement to this hypothesis is the effect of neighboring pedestrians due to space constraints (e.g., collision avoidance [36]) and other cognitive coupling between neighbors [46]. From a mechanical perspective, the most significant and plausible complement to the energy optimality hypothesis is the hypothesis that the observed human-platform dynamics is an emergent property of the controller that keeps human walking stable. While limited theoretical explorations [7,36] have found evidence for the stability hypothesis, a definitive understanding of the human-platform dynamics has to await a more detailed characterization of the controller that maintains stability during walking — an outstanding open problem in locomotion biomechanics [10,11,47]. Once we have this human walking controller, we could check if one or many biped models endowed with such a stabilizing controller, walking forward on a shaky bridge, automatically synchronize with each other and to the bridge, thereby causing large bridge oscillations. Given that energy optimality has been so successful in explaining other aspects of human movement and can at least explain some known qualitative features of humans on moving surfaces, we need careful studies that can distinguish energetic optimality from stability. For instance, it may superficially be thought that a wider step width is an indication that the humans are stability-challenged in the lateral direction; however, our calculations show that wider step width is energy optimal even when stability is not taken into account; thus, delineating the individual effects of energetics and stability might be non-trivial.

Appendix

The appendix contains the following three sections:

- **Section A1** lists the equations of motion for all variants of the simple model described in figure 1 of the main manuscript. These variants are the parameterised-leg-force model and the inverted pendulum model, each of which may be coupled with an infinite or finite inertia platform.
- **Section A2** details each term in the cost function for the biped as described in section 1 of the main manuscript.
- **Section A3** provides specific information about the ODE solver and optimisation algorithms used in our calculations.

A1. Equations of motion

Body motion. For the model shown in figure 1, there are two forces acting on the center of mass during single stance, namely, the force along the leg F and the weight of the biped $m_{\rm com}g$. The forward, vertical and lateral positions of the body center of mass (CoM) and the stance foot in contact with the ground are represented as x, y and z respectively with appropriate subscripts. The leg length is ℓ, given by,

$$\ell^2 = (x_{\rm com} - x_{\rm foot})^2 + (y_{\rm com} - y_{\rm foot})^2 + (z_{\rm com} - z_{\rm foot})^2 \,. \tag{A1.1}$$

The equations of motion for the center of mass are:

$$m_{\rm com}\ddot{x}_{\rm com} = F\,\frac{x_{\rm com} - x_{\rm foot}}{\ell}, \tag{A1.2}$$

$$m_{\rm com}\ddot{y}_{\rm com} = F\,\frac{y_{\rm com} - y_{\rm foot}}{\ell} - m_{\rm com}g, \text{ and} \tag{A1.3}$$

$$m_{\rm com}\ddot{z}_{\rm com} = F\,\frac{z_{\rm com} - z_{\rm foot}}{\ell}, \tag{A1.4}$$

which are applicable for all versions of the biped model.

Non-dimensionalization Non-dimensionalization is performed by dividing by appropriate combinations of mass $m_{\rm com}$, maximum leg length $\ell_{\rm max}$, and acceleration due to gravity g. In the following, we denote the non-dimensional analogs of dimensional quantities by adding an overbar; for instance, fore-aft position $\bar{x}_{\rm com} = x_{\rm com}/\ell_{\rm max}$, non-dimensional leg force $\bar{F} = F/(m_{\rm com}g)$, non-dimensional speed $\bar{v} = v/\sqrt{g\ell_{\rm max}}$, and non-dimensional time $\bar{t} = t\sqrt{g/\ell_{\rm max}}$. Energy cost per distance is normalized by mg, energy cost per unit time is normalized by $mg\sqrt{g\ell_{\rm max}}$, and energy per step is normalized by $mg\ell_{\rm max}$.

Platform motion. When we have a finite inertia platform, we add another equation for the motion of the platform in the lateral direction:

$$m_{\rm platform}\ddot{z}_{\rm platform} + B_{\rm platform}\dot{z}_{\rm platform} + K_{\rm platform}z_{\rm platform} = -F\,\frac{z_{\rm com} - z_{\rm foot}}{\ell} \tag{A1.5}$$

where $K_{\rm platform}$ and $B_{\rm platform}$ are the stiffness and damping of the platform in the lateral direction, respectively. For the infinite inertia platform, the platform motion is specified as sinusoidal, of the form:

$$z_{\rm platform} = A_{\rm platform}\sin\left(\omega_{\rm platform}t + \phi\right) \tag{A1.6}$$

where $A_{\rm platform}$ is the amplitude, $\omega_{\rm platform}$ is the frequency of oscillation, and ϕ is the phase difference between the biped stride and the platform oscillation.

Leg forces. We performed two different types of optimisation calculations: (1) in which the leg forces are allowed to be arbitrary and (2) in which the biped performs an inverted pendulum gait with push-off and heel-strike impulses. When the leg force is arbitrary, they are parameterized as piecewise linear $F(t)$ to be computed by the optimizer. When the biped is assumed to perform an exact 3D inverted pendulum motion, we use a differential algebraic equation formulation to enforce the leg length constraint. We do not fix the leg length, but rather constrain the motion of the center of mass to be such that the leg length cannot change from the beginning of the motion. The second derivative of this leg length constraint (equation A1.1) produces the following additional ODE:

$$\begin{aligned}(x_{\rm com}-x_{\rm foot})\,\ddot{x}_{\rm com}+(y_{\rm com}-y_{\rm foot})\,\ddot{y}_{\rm com}+(z_{\rm com}-z_{\rm foot})\,\ddot{z}_{\rm com}=\\ -\dot{x}_{\rm com}^2-\dot{y}_{\rm com}^2-\left(\dot{z}_{\rm com}^2-\dot{z}_{\rm platform}^2\right)^2+\ddot{z}_{\rm platform}\,(z_{\rm com}-z_{\rm foot})\,.\end{aligned} \tag{A1.7}$$

This equation, along with the equations A1.2-A1.4 can be combined to determine the acceleration of the center of mass and the force along the leg. For the finite inertia platform, we add equation A1.5 to these equations to get the lateral acceleration of the platform as well.

Model parameters. For the finite inertia platform, the nominal values of mass, stiffness, and damping are identical to those used in [4] as approximating the London Millennium Bridge: $M=1.13\times10^5$ kg, $B_{\rm platform}=1.1\times10^4$ Nsm^{-1}, and $K_{\rm platform}=4.73\times10^6$ Nm^{-1}. We also used human mass $m=70$ kg, maximum leg length $\ell_{\max}=0.95$ m, and $g=9.81$ ms^{-1}.

A2. Metabolic cost model

The cost function contains the following four terms, resting metabolic rate, stance work cost, stance force cost, and swing leg cost, defined as follows:

(i) **Resting metabolic rate.** The experimentally determined metabolic cost of walking [48] for a human at a given speed of walking v is:

$$\text{Metabolic rate per unit mass}=\left(2.2+1.155\left(\frac{v}{1\text{ ms}^{-1}}\right)^2\right)\text{ Watts per kg}. \tag{A2.1}$$

Of this, roughly 1.4 Watts per kg is the resting metabolic rate [48]. Converting this resting rate to the appropriate non-dimensional units and multiplying by the mass of the biped gives us the resting metabolic rate for the biped. The resting metabolic rate is key to obtaining a non-zero optimal speed [14]; given a finite resting rate, infinitesimal walking speeds would imply very large costs for traveling a given distance.

(ii) **Stance work cost.** Humans are known to perform positive work at an average efficiency of approximately 25% ($\eta_{\rm pos}=0.25$) and negative work at an efficiency of 120% ($\eta_{\rm neg}=1.2$) [23,31]. We determine the stance cost as a linear combination of negative and positive work, $W_{\rm neg}$ and $W_{\rm pos}$, done by the leg on the center of mass, using the reciprocal efficiency as the weighing parameter.

$$\text{Stance work cost}=\frac{1}{\eta_{\rm pos}}W_{\rm pos}+\frac{1}{\eta_{\rm neg}}W_{\rm neg}. \tag{A2.2}$$

When the biped is controlled with arbitrary parameterized leg forces $F(t)$, the positive and negative stance work is computed by integrating the positive and negative part of the power $P=F\dot{\ell}$ produced by the leg over the course of the motion:

$$W_{\rm pos}=\int\lceil P\rceil^+dt\ \text{ and }W_{\rm neg}\ =\int\lceil -P\rceil^+dt, \tag{A2.3}$$

where $\lceil P\rceil^+$ is the positive part: $\lceil P\rceil^+=P$ when $P\geq0$ and $\lceil P\rceil^+=0$ when $P<0$.
For the inverted pendulum version of the biped, the work done by the leg on the center of mass is entirely condensed into the push-off and heel-strike impulses; the expressions

in equation A2.3 will evaluate to exactly zero during the inverted pendulum phase (leg length does not change, therefore the leg does zero work on the center of mass). The work done by each of these impulses, which is entirely positive for push-off and entirely negative for heel-strike, equals the kinetic energy change produced by them in the pedestrian-platform system (see [31,35] or supplementary information [26]):

$$\begin{aligned}\text{Kinetic energy change} \quad &= \left(\tfrac{m_{\text{com}}}{2} v_{\text{com}}^2 + \tfrac{m_{\text{platform}}}{2} v_{\text{platform}}^2\right)_{\text{after-impulse}} \\ &\quad - \left(\tfrac{m_{\text{com}}}{2} v_{\text{com}}^2 + \tfrac{m_{\text{platform}}}{2} v_{\text{platform}}^2\right)_{\text{before-impulse}}.\end{aligned}$$

(iii) **Swing leg cost.** The cost of moving the swing leg is determined as the weighted sum of the positive and negative work needed to move the foot from its position during one stance phase to its next position, starting and ending at rest. For this work calculation, the velocity of the swing leg, v_{swing}, is taken as the ratio of distance between the positions of the foot in two consecutive steps and the step period. Both positive and negative work equal an effective leg kinetic energy $m_{\text{foot}} v_{\text{swing}}^2$ during swing; we use an effective foot mass $m_{\text{foot}} = 0.05 m_{\text{com}}$ as in [26] so as to approximate the moment of inertia of the entire leg with the point-foot. Swing cost equals this kinetic energy scaled by the reciprocal efficiencies $(1/\eta_{\text{pos}} + 1/\eta_{\text{neg}})$.
This simplified swing cost we used does not go to zero nor is a minimum at the legÕs natural frequency, but instead monotonically increases with swing amplitude and frequency. So, we rule out the possibility of leg swing cost reduction by walking close to the passive leg swing frequency. It has been argued that in normal walking, humans walk at higher frequencies than passive leg swing (as do our models' optima) so as to have smaller step lengths and smaller stance work costs [29]; that is, the presence of swing cost prevents the optimal stride frequency going to infinity – as large stride frequencies and small step lengths reduce the stance work cost.

(iv) **Stance force cost.** This is a cost proportional to the time-integral of the force along the leg.

$$\text{Stance Force Cost} = \eta_{\text{force}} \int F \, dt. \tag{A2.4}$$

We obtain the proportionality factor η_{force} by noting that subtracting the resting metabolic rate from equation A2.1 predicts a non-zero metabolic rate for zero walking speed. As a simplifying assumption, we attribute this difference, not explainable using stance or swing work, to the integral of the leg force. We use non-dimensional $\bar{\eta}_{\text{force}} = 0.026$. The stance force cost penalizes large step widths and large step lengths.

The sum of these four cost terms per unit distance is used as the objective function to be minimized in our optimisation calculations. The non-dimensional version of this objective function is an estimate of the "cost of transport" of walking [49,50].

A3. Details of the numerical optimisation

As noted before, we performed two different types of optimisations, one in which the leg forces and length changes are allowed to be arbitrary (force-parameterized version) and one in which the walking is assumed to be inverted pendulum. We performed these two types of optimisations for both the infinite inertia platform and the finite inertia platform situations. Instead of describing all these four calculations, we describe two of them: how we minimize the metabolic energy based cost function for a force-parameterised biped model walking on an infinite-inertia platform and for an inverted pendulum biped model walking on a finite-inertia platform. The other two optimisations, namely force-parameterized version for finite inertia and inverted pendulum version for infinite inertia are completely analogous. Overall, we use similar methods to those used in our previous work in biped optimisations [21,23]; see, especially, supplementary material of [23] for further technical details.

Force-parameterized optimisation for walking on an infinite inertia platform. For the force-parameterised biped model, for each calculation, we fix the step period t_{step}, walking speed v_{step}, the platform oscillation amplitude A, the platform oscillation period $t_{\text{platform}} = 2t_{\text{step}}$ by assumption of entrainment, from which we determine the platform oscillation frequency ω. The rest of the model is defined by the initial position and velocity of the center of mass $(x_{\text{com0}}, y_{\text{com0}}, z_{\text{com0}})$ and $(\dot{x}_{\text{com0}}, \dot{y}_{\text{com0}}, \dot{z}_{\text{com0}})$ for each step, the position of the foot during the second step $(x_{\text{foot2}}, 0, z_{\text{foot2}})$, the relative phase of the platform motion and the ϕ and $2N + 2$ elements of a piece-wise linear force curve F ($N_{\text{segments}} + 1$ for each step). The position of the foot during the first step is the origin, without loss of generality. This gives us $2N_{\text{segments}} + 17$ parameters of a gait:

$$\mathbb{Z} = \left(t_{\text{step}}, v_{\text{step}}, \omega, A, x_{\text{CoM0}}, y_{\text{com0}}, z_{\text{com0}}, \dot{x}_{\text{com0}}, \dot{y}_{\text{com0}}, \dot{z}_{\text{com0}}, \phi, x_{\text{foot2}}, z_{\text{foot2}}, F_j\right)$$

with $j = 1, \ldots, 2N_{\text{segments}} + 2$. As noted, five out of these $2N_{\text{segments}} + 17$ are fixed for each calculation and therefore, the rest $2N_{\text{segments}} + 12$ quantities are unknowns decided by the optimisation. The gait is divided into $2N_{\text{segments}}$ grid segments, separated by the grid-points at which the leg forces are specified; the body motion in each segment is obtained by integrating the appropriate ODEs, with each integration using the end state of previous grid segment as the initial state.

This walking gait is subject to the following constraints:

- A leg length inequality, $\ell \leq \ell_{\max}$, imposed by evaluating the leg length for at least 3 points in each grid segment. Since $\ell_{\max}$ is used for normalization, we have $\ell_{\max} = 1$.
- Periodicity constraints requiring that the state at the end of the second step is equal to the state at the beginning of the first step except for a forward translation equal to the stride length (d_{stride}) in the x direction: $d_{\text{stride}} = 2v_{\text{step}}t_{\text{step}}$, $x_{\text{com}}(2t_{\text{step}}) = x_{\text{com0}} + d_{\text{stride}}$, $y_{\text{com}}(2t_{\text{step}}) = y_{\text{com0}}$, $z_{\text{com}}(2t_{\text{step}}) = z_{\text{com0}}$, $\dot{x}_{\text{com}}(2t_{\text{step}}) = \dot{x}_{\text{com0}}$, $\dot{y}_{\text{com}}(2t_{\text{step}}) = \dot{y}_{\text{com0}}$, and $\dot{z}_{\text{com}}(2t_{\text{step}}) = \dot{z}_{\text{com0}}$.
- The forces are bounded $0 \leq F_j \leq F_{\max}$ for $j = 1, \ldots, 2N_{\text{segments}} + 2$ to ensure that the foot does not pull on the ground and the leg force magnitude is reasonable. We used $\bar{F}_{\max} = F/F_{\max} = 4$; none of the qualitative results change if we used $\bar{F}_{\max} = 3$ or 5.
- The initial states and the position of the foot during the second step are bounded within a sufficiently large box. For example $-l_{\max} \leq x_{\text{com0}} \leq l_{\max}$. These bounds are never active at the optimal solution.

Inverted pendulum optimisation for walking on a finite inertia platform. For each optimisation with inverted-pendulum model on a finite inertia platform, we fix the mass m_{platform}, stiffness K_{platform} and damping constant B_{platform} for the platform and the number of pedestrians $N_{\text{pedestrians}}$. The rest of the model is defined by the step period t_{step}, the step length d_{step}, the initial position and velocity of the center of mass $(x_{\text{com10}}, y_{\text{com10}}, z_{\text{com10}})$ and $(\dot{x}_{\text{com10}}, \dot{y}_{\text{com10}}, \dot{z}_{\text{com10}})$, the initial lateral position and velocity of the platform $z_{\text{platform10}}$ and $\dot{z}_{\text{platform10}}$, the initial position and velocity of the center of mass for the second step $(x_{\text{com20}}, y_{\text{com20}}, z_{\text{com20}})$ and $(\dot{x}_{\text{com20}}, \dot{y}_{\text{com20}}, \dot{z}_{\text{com20}})$, the initial lateral position and velocity of the platform during the second step $z_{\text{platform20}}$ and $\dot{z}_{\text{platform20}}$, the position of the foot during the second step (x_{foot2}, 0, z_{foot2}), and the magnitudes of the four impulses $I_{\text{push-off1}}$, $I_{\text{heel-strike1}}$, $I_{\text{push-off2}}$ and $I_{\text{heel-strike2}}$. The foot position during the first step as the origin for the system. This gives us 28 parameters to define the gait $\mathbb{Z}$ = (m_{platform}, K_{platform}, B_{platform}, t_{step}, d_{step}, x_{com10}, y_{com10}, z_{com10}, $\dot{x}_{\text{com10}}$, $\dot{y}_{\text{com10}}$, $\dot{z}_{\text{com10}}$, x_{com20}, y_{com20}, z_{com20}, $\dot{x}_{\text{com20}}$, $\dot{y}_{\text{com20}}$, $\dot{z}_{\text{com20}}$, $z_{\text{platform10}}$, $\dot{z}_{\text{platform10}}$, $z_{\text{platform20}}$, $z_{\text{platform20}}$, x_{foot2}, z_{foot2}, $I_{\text{push-off1}}$, $I_{\text{heel-strike1}}$, $I_{\text{push-off2}}$, $I_{\text{heel-strike2}}$), out of which 4 are fixed constants during a given optimisation.

The gait is divided into two sections, one for each step. The initial point of a step is subject to a heel-strike impulse, which changes the velocity of the biped and the platform. This heel-strike impulse is calculated to ensure that the leg-length-rate after impulse is exactly 0 to allow for inverted pendulum walking. The resulting state is integrated using the ODE for the inverted

pendulum model and finally this state is subject to a push-off impulse to produce the end state for the section. The heel-strike impulse needed to make leg-length rate 0 at any point of time can be determined using the following equation:

$$I_{\mathrm{heel-strike}} = -\frac{\dot{x}_{\mathrm{com}}(x_{\mathrm{com}} - x_{\mathrm{foot}}) + \dot{y}_{\mathrm{com}}(y_{\mathrm{com}} - y_{\mathrm{foot}}) + (\dot{z}_{\mathrm{com}} - \dot{z}_{\mathrm{foot}})(z_{\mathrm{com}} - z_{\mathrm{foot}})}{\frac{(x_{\mathrm{com}}-x_{\mathrm{foot}})^2}{m\ell} + \frac{(y_{\mathrm{com}}-y_{\mathrm{foot}})^2}{m\ell} + \frac{(m+m_{\mathrm{platform}})(z_{\mathrm{com}}-z_{\mathrm{foot}})^2}{m m_{\mathrm{platform}}\ell}} \tag{A3.1}$$

The optimisation problem is solved subject to the following constraints:

- A leg length equality, $\ell = \ell_{\max}$ imposed by evaluating the leg length at the beginning of each step; in non-dimensional terms, $\ell/\ell_{\max} = 1$. If the constraint is met at the beginning of the step, the fact that the impulses can only change velocity and that the motion is inverted-pendulum-like ensure that it shall be met till the end of the step.
- Periodicity constraints requiring that the state at the end of the second step is equal to the state at the beginning of the first step except for a forward translation equal to the stride length d_{stride} in the x-direction: $d_{\mathrm{stride}} = 2d_{\mathrm{step}}$. $x_{\mathrm{com}}(2t_{\mathrm{step}}) = x_{\mathrm{com10}} + d_{\mathrm{stride}}$, $y_{\mathrm{com}}(2t_{\mathrm{step}}) = y_{\mathrm{com10}}$, $z_{\mathrm{com}}(2t_{\mathrm{step}}) = z_{\mathrm{com10}}$, $\dot{x}_{\mathrm{com}}(2t_{\mathrm{step}}) = \dot{x}_{\mathrm{com10}}$, $\dot{y}_{\mathrm{com}}(2t_{\mathrm{step}}) = \dot{y}_{\mathrm{com10}}$, $\dot{z}_{\mathrm{com}}(2t_{\mathrm{step}}) = \dot{z}_{\mathrm{com10}}$, $z_{\mathrm{platform}}(2t_{\mathrm{step}}) = z_{\mathrm{platform10}}$, and $\dot{z}_{\mathrm{paltform}}(2t_{\mathrm{step}}) = \dot{z}_{\mathrm{platform10}}$.
- Continuity constraints requiring that the state at the end of the first step is equal to the state at the beginning of the second step $x_{\mathrm{com}}(t_{\mathrm{step}}) = x_{\mathrm{com20}}$, $y_{\mathrm{com}}(t_{\mathrm{step}}) = y_{\mathrm{com20}}$, $z_{\mathrm{com}}(t_{\mathrm{step}}) = z_{\mathrm{com20}}$, $\dot{x}_{\mathrm{com}}(t_{\mathrm{step}}) = \dot{x}_{\mathrm{com20}}$, $\dot{y}_{\mathrm{com}}(t_{\mathrm{step}}) = \dot{y}_{\mathrm{com20}}$, $\dot{z}_{\mathrm{com}}(t_{\mathrm{step}}) = \dot{z}_{\mathrm{com20}}$, $z_{\mathrm{platform}}(t_{\mathrm{step}}) = z_{\mathrm{platform20}}$, and $\dot{z}_{\mathrm{paltform}}(t_{\mathrm{step}}) = \dot{z}_{\mathrm{platform20}}$.
- The impulses are bounded $0 \le I_j \le I_{\max}$ to ensure that the foot does not pull on the ground and the impulse magnitude is reasonable. The impulse upper bound in never active in the optimal solutions, so its exact value is irrelevant.
- The forces are bounded $0 \le F_j \le F_{\max}$ to ensure that the foot does not pull on the ground and the leg force magnitude is reasonable. This is done by calculating the force at sufficiently many intermediate point of the gait using the equations of motion. The upper bound on the force is never active in the optimal solutions, so its exact value is irrelevant.

Computational solution. The equations of motion were solved using `ode45` in `MATLAB` with absolute and relative tolerances of at most 10^{-9} and also an equivalent constant step-size Runge-Kutta method for consistency. Optimisation was performed with `SNOPT` [51,52], a robust constrained nonlinear optimisation program; we used optimality and feasibility tolerances of 10^{-6}. The parameterised-leg-force biped model used at piece-wise linear forces with at least 14 segments to simulate each step of walking.

The planar inverted pendulum walking solution is obtained robustly by the optimisation from random initial seeds far away from the optimum, when the platform is constrained to not move (essentially a repetition of calculations elsewhere [21,23]). When the platform is moved or the bridge is allowed to move, to obtain the non-planar optimal solutions, we typically started the optimisations from initial seeds that are sufficiently perturbed versions of the planar solution. When we obtain optimal solutions for a sequence of parameter values, we use the optimal solution for the previous parameter value as the initial seed for the current parameter value – and then do a forward and backward sweep of the parameter values to pick the lower of the two optimal solutions. Numerical experiments suggested that there were at most two local minima, the planar walking optimum and the non-planar walking optimum, and sometimes only one; we did not see evidence for many more local minima. While we cannot rule out that there does not exist a lower global minimum, we have reliably demonstrated that lower-than-planar costs are achievable with non-planar walking.

Ethics statement. This work did not involve any active collection of human data, but only computer simulations of human behavior.

Data accessibility statement. This work does not have any experimental data.

Competing interests statement. We have no competing interests.

Authors' contributions. V.J. and M.S. conceived the mathematical models, interpreted the computational results and wrote the paper. V.J. implemented and performed most of the simulations and optimization calculations, partly in discussion with M.S. All authors gave final approval for publication.

Funding. This work was supported by National Science Foundation grant 1254842.

References

1. D. P. Ferris, M. Louie, and C. T. Farley, "Running in the real world: adjusting leg stiffness for different surfaces," *Proc. Roy. Soc. B*, vol. 265, no. 1400, pp. 989–994, 1998.
2. T. M. Lejeune, P. A. Willems, and N. C. Heglund, "Mechanics and energetics of human locomotion on sand," *J. Exp. Biol.*, vol. 201, no. 13, pp. 2071–2080, 1998.
3. P. Dallard, A. J. Fitzpatrick, A. Flint, S. Le Bourva, A. Low, R. M. Ridsdill Smith, and M. Willford, "The London Millennium Footbridge," *The Structural Engineer*, vol. 79, no. 22, pp. 17–33, 2001.
4. S. H. Strogatz, D. M. Abrams, A. McRobie, B. Eckhardt, and E. Ott, "Theoretical mechanics: crowd synchrony on the millennium bridge," *Nature*, vol. 438, pp. 43–4, Nov. 2005.
5. H. Bachmann and W. Ammann, *Vibrations in structures: induced by man and machines*. IABSE Structural Engineering Documents, no. 3e. Zurich, Switzerland: IABSE, 1987.
6. Y. Fujino, B. M. Pacheco, S. Nakamura, and P. Warnitchai, "Synchronization of human walking observed during lateral vibration of a congested pedestrian bridge," *Earthquake Eng. Struct. Dyn.*, vol. 22, pp. 741–758, 1993.
7. J. H. G. Macdonald, "Lateral excitation of bridges by balancing pedestrians," *Proc. R. Soc. A*, vol. 465, pp. 1055–1073, Dec. 2008.
8. S. P. Carroll, J. S. Owen, and M. F. M. Hussein, "Reproduction of lateral ground reaction forces from visual marker data and analysis of balance response while walking on a laterally oscillating deck," *Engineering Structures*, vol. 49, pp. 1034–1047, Apr. 2013.
9. J. C. Dean, N. B. Alexander, and A. D. Kuo, "The effect of lateral stabilization on walking in young and old adults," *IEEE Trans Biomed Eng*, vol. 54, no. 11, pp. 1919–1926, 2007.
10. A. L. Hof, S. M. Vermerris, and W. A. Gjaltema, "Balance responses to lateral perturbations in human treadmill walking," *J. Exp. Biol.*, vol. 213, no. 15, pp. 2655–2664, 2010.
11. Y. Wang and M. Srinivasan, "Stepping in the direction of the fall: the next foot placement can be predicted from current upper body state in steady state walking," *Biology Letters (accepted)*, 2014.
12. P. Högberg, "How do stride length and stride frequency influence the energy-output during running?," *Arbeitsphysiologie*, vol. 14, pp. 437–441, 1952.
13. H. J. Ralston, "Energy-speed relation and optimal speed during level walking," *Eur J Appl Physiol (Int. Z. angew. Physiol. einsehl. Arbeitsphysiol)*, vol. 17, pp. 277–283, 1958.
14. M. Srinivasan, "Optimal speeds for walking and running, and walking on a moving walkway," *CHAOS*, vol. 19, p. 026112, 2009.
15. J. M. Donelan, R. Kram, and A. D. Kuo, "Mechanical and metabolic determinants of the preferred step width in human walking.," *Proc. R. Soc. Lond. B*, vol. 268, pp. 1985–1992, 2001.
16. L. L. Long and M. Srinivasan, "Walking, running, and resting under time, distance, and average speed constraints: optimality of walk–run–rest mixtures," *Journal of The Royal Society Interface*, vol. 10, no. 81, p. 20120980, 2013.
17. R. M. Alexander, "Optimum walking techniques for quadrupeds and bipeds.," *J. Zool., Lond.*, vol. 192, pp. 97–117, 1980.
18. R. M. Alexander, "Optimization and gaits in the locomotion of vertebrates.," *Physiol. Rev.*,, vol. 69, pp. 1199–1227, 1989.
19. A. E. Minetti and R. M. Alexander, "A theory of metabolic costs for bipedal gaits," *J. Theor. Biol*, vol. 186, pp. 467–476, 1997.

20. F. C. Anderson and M. G. Pandy, "Dynamic optimization of human walking," *Journal of Biomechanical Engineering*, vol. 123, pp. 381–390, 2001.
21. M. Srinivasan and A. Ruina, "Computer optimization of a minimal biped model discovers walking and running.," *Nature*, vol. 439, pp. 72–75, 2006.
22. M. Ackermann and A. J. van den Bogert, "Optimality principles for model-based prediction of human gait," *Journal of Biomechanics*, vol. 43, p. 1055Ð1060, 2010.
23. M. Srinivasan, "Fifteen observations on the structure of energy-minimizing gaits in many simple biped models.," *J. Royal Society, Interface*, vol. 8, pp. 74–98, Jan. 2011.
24. J. M. Wang, S. R. Hamner, S. L. Delp, and V. Koltun, "Optimizing locomotion controllers using biologically-based actuators and objectives," *ACM Transactions on Graphics (Proc. SIGGRAPH)*, vol. 31, 25, 2012.
25. R. H. Miller, "A comparison of muscle energy models for simulating human walking in three dimensions," *J. Biomech.*, vol. 47, no. 6, pp. 1373–1381, 2014.
26. M. L. Handford and M. Srinivasan, "Sideways walking: preferred is slow, slow is optimal, and optimal is expensive," *Biol. Lett.*, vol. 10, p. 20131006, 2014.
27. J. M. Finley, A. J. Bastian, and J. S. Gottschall, "Learning to be economical: the energy cost of walking tracks motor adaptation," *J. Physiol.*, vol. 591, pp. 1081–1095, 2013.
28. J. E. A. Bertram and A. Ruina, "Multiple walking speed–frequency relations are predicted by constrained optimization," *J. theor. Biol.*, vol. 209, no. 4, pp. 445–453, 2001.
29. A. D. Kuo, "A simple model of bipedal walking predicts the preferred speed–step length relationship," *J. biomech. Engg.*, vol. 123, no. 3, pp. 264–269, 2001.
30. R. M. Alexander, "Mechanics of bipedal locomotion," *Perspectives in Experimental Biology*, vol. 1, pp. 493–504, 1976.
31. A. D. Kuo, J. M. Donelan, and A. Ruina, "Energetic consequences of walking like an inverted pendulum: step-to-step transitions.," *Exercise and sport sciences reviews*, vol. 33, pp. 88–97, Apr. 2005.
32. H. Geyer, A. Seyfarth, and R. Blickhan, "Compliant leg behaviour explains basic dynamics of walking and running.," *Proc. R. Soc. B.*, vol. 273, pp. 2861–7, Nov. 2006.
33. M. Srinivasan and P. Holmes, "How well can spring-mass-like telescoping leg models fit multi-pedal sagittal-plane locomotion data?," *Journal of Theoretical Biology*, vol. 255, pp. 1–7, 2008.
34. D. V. Lee, J. E. A. Bertram, J. T. Anttonen, I. G. Ros, S. L. Harris, and A. A. Biewener, "A collisional approach to quadrupedal gait dynamics," *J. R. Soc. Interface*, vol. 8, pp. 1480–1486, 2011.
35. A. Ruina, J. E. A. Bertram, and M. Srinivasan, "A collisional model of the energetic cost of support work qualitatively explains leg-sequencing in walking and galloping, pseudo-elastic leg behavior in running and the walk-to-run transition.," *J. Theor. Biol.*, vol. 14, pp. 170–192, 2005.
36. S. Carroll, J. Owen, and M. Hussein, "A coupled biomechanical/discrete element crowd model of crowd-bridge dynamic interaction and application to the Clifton Suspension Bridge," *Engineering Structures*, vol. 49, pp. 58–75, Apr. 2013.
37. B. T. Peters, R. A. Brady, and J. J. Bloomberg, "Walking on an Oscillating Treadmill: Strategies of Stride-Time Adaptation," *Ecological Psychology*, vol. 24, no. 614, pp. 265–278, 2012.
38. J. Ahn and N. Hogan, "Walking is not like reaching: evidence from periodic mechanical perturbations," *PloS one*, vol. 7, no. 3, p. e31767, 2012.
39. M. Snaterse, R. Ton, A. D. Kuo, and J. M. Donelan, "Distinct fast and slow processes contribute to the selection of preferred step frequency during human walking," *Journal of Applied Physiology*, vol. 110, no. 6, pp. 1682–1690, 2011.
40. S. M. O'Connor and J. M. Donelan, "Fast visual prediction and slow optimization of preferred walking speed," *Journal of neurophysiology*, vol. 107, no. 9, pp. 2549–2559, 2012.
41. S. K. S. Thorpe, R. L. Holder, and R. H. Crompton, "Origin of human bipedalism as an adaptation for locomotion on flexible branches," *Science*, vol. 316, pp. 1328–1331, 2007.
42. S. K. S. Thorpe, R. H. Crompton, and R. M. Alexander, "Orangutans use compliant branches to lower the energetic cost of locomotion," *Biology Letters*, vol. 3, pp. 253–256, 2007.
43. A. E. Kerdok, A. A. Biewener, T. A. McMahon, P. G. Weyand, and H. M. Herr, "Energetics and mechanics of human running on surfaces of different stiffnesses," *J. Appl. Physiol.*, vol. 92, pp. 469–478, 2002.
44. H. Weimerskirch, J. Martin, Y. Clerquin, P. Alexandre, and S. Jiraskova, "Energy saving in flight formation," *Nature*, vol. 413, no. 6857, pp. 697–698, 2001.

45. J. Herskin and J. F. Steffensen, "Energy savings in sea bass swimming in a school: measurements of tail beat frequency and oxygen consumption at different swimming speeds," *J. Fish Biol.*, vol. 53, no. 2, pp. 366–376, 1998.
46. J. Wagnild and C. M. Wall-Scheffler, "Energetic consequences of human sociality: Walking speed choices among friendly dyads," *PloS one*, vol. 8, no. 10, p. e76576, 2013.
47. C. E. Bauby and A. D. Kuo, "Active control of lateral balance in human walking," *J. Biomech.*, vol. 33, pp. 1433–1440, 2000.
48. A. C. Bobbert, "Energy expenditure in level and grade walking," *Journal of Applied Physiology*, vol. 15, no. 6, pp. 1015–1021, 1960.
49. V. A. Tucker, "Energetic cost of locomotion in animals," *Comparative Biochemistry and Physiology*, vol. 34, no. 4, pp. 841–846, 1970.
50. S. Collins, A. Ruina, R. Tedrake, and M. Wisse, "Efficient bipedal robots based on passive-dynamic walkers," *Science*, vol. 307, no. 5712, pp. 1082–1085, 2005.
51. P. E. Gill, W. Murray, and M. A. Saunders, "Snopt: An sqp algorithm for large-scale constrained optimization.," *SIAM J.Optim.*, vol. 12, pp. 979–1006, 2002.
52. K. Holmstrom *et al.*, "The tomlab optimization environment in matlab," 1999.

Supplementary Appendix for

Walking on a moving surface: Energy-optimal walking motions on a shaky bridge and a shaking treadmill reduce energy costs below normal

Varun Joshi and Manoj Srinivasan
Mechanical and Aerospace Engineering, Columbus, OH - 43201
joshi.142@osu.edu, srinivasan.88@osu.edu, http://movement.osu.edu

The supplementary information for this manuscript contains:

1. **A Supplementary Appendix** containing thirteen figures (this document), figures S1 to S13 providing additional technical information about the optimal walking motions under different situations and assumptions.
2. **Two supplementary videos**, one showing the optimal walking motions on a shaking treadmill and another showing optimal walking motions on a shakeable bridge, with and without shaking. Note that in these videos, the swing leg is shown for clarity; as we do not explicitly simulate swing leg dynamics, the swing leg motion is depicted as having uniform speed.

Figure S1 shows two different optimal walking solutions on an infinite inertia platform oscillated externally: one solution with non-zero leg work and another with zero leg work. Figure S2 shows the optimal body motion on a shaky bridge, partly providing an alternative representation of figure 4 of the main manuscript. Figures S3-S6 depict the variation of metabolic cost per unit distance, platform oscillation amplitude, pedestrian stride frequency, walking speed and step-width with increasing number of pedestrians for various calculations for walking on the finite inertia platform. Figures S3 and S4 show this variation for a range of platform stiffness and a fixed platform damping. Figure S5 shows the variation of these parameters for fixed platform stiffness and varying platform damping. Figure S6 shows the same calculation with a minimum step-width constraint on the gait. Figure S7 shows that the inverted pendulum solution is optimal for a force-parameterized model of the biped walking on the finite-inertia bridge. Figures S8 and S9 show that solution trends do not change significantly for either the infinite-inertia or the finite-inertia calculation, when we change model parameters such as foot mass, resting rate, integral of force multiplier η_{force}, or the walking speed. Figures S10, S11, and S12 show effect of oscillations on the individual components of cost in the finite inertia bridge case. Figure S13 shows the individual cost components for the infinite-inertia treadmill case.

All physical quantities in the figures in this Supplementary Appendix are non-dimensional.

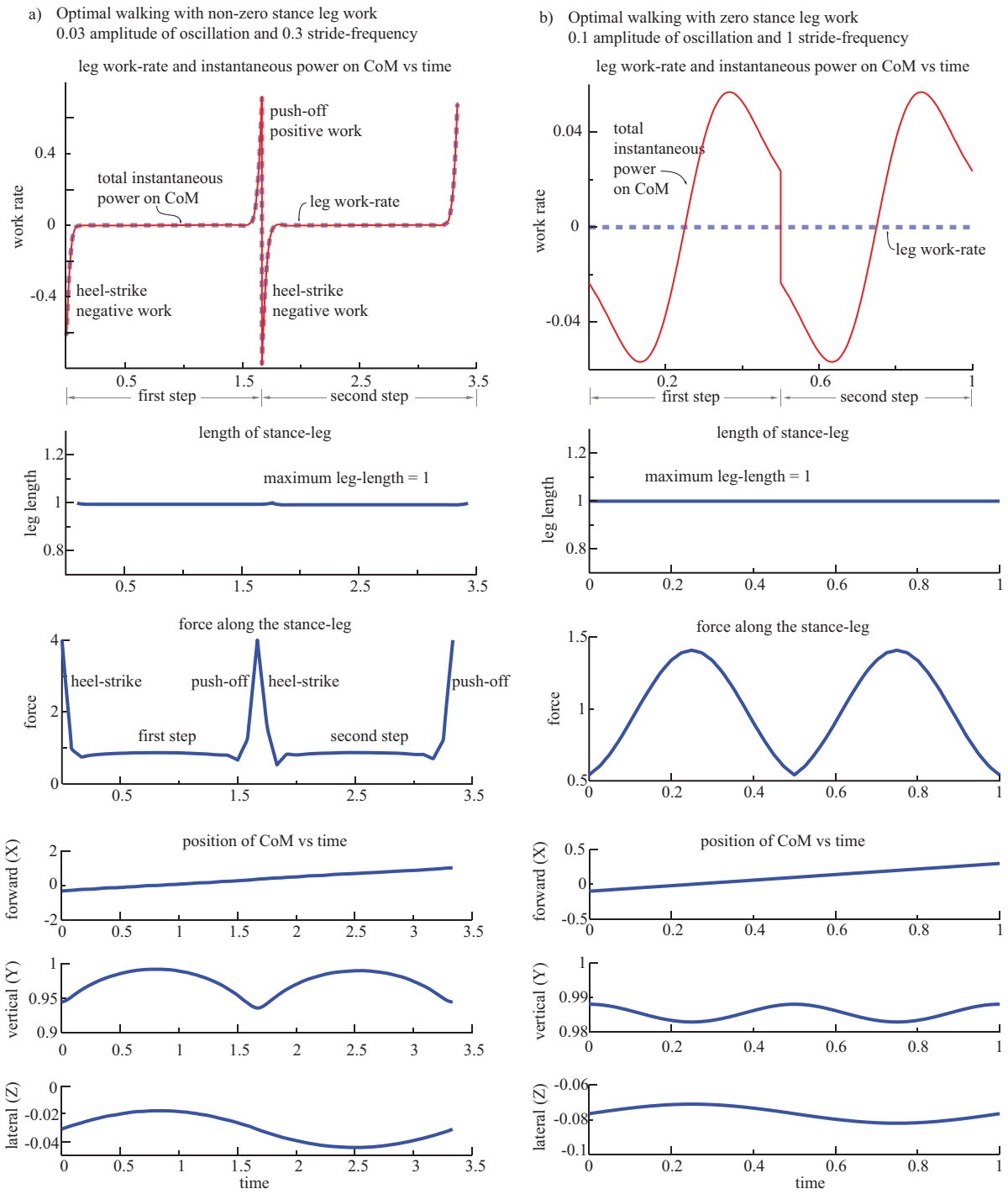

Figure S1: Optimal walking motion on infinite inertia platform, for force-parameterized optimisations. These figures show the optimal solution on a platform oscillating sideways sinusoidally under two different oscillation conditions. In both cases the pedestrian is constrained to walk at a non-dimensional speed of 0.4 ≈ 1.2 m/s. a) Non-dimensional stride-frequency equals 0.3 and platform oscillation amplitude equals 0.03. We see that the solutions take the form of 3D inverted pendulum walking, in which the leg length is constant for most of stance phase, except during two brief periods, a heel-strike impulse performing negative work at the beginning of stance phase and a push-off impulse performing positive work at the end of stance phase. b) Non-dimensional stride-frequency equals 1 and platform oscillation amplitude is 0.1. The solution continues to be inverted pendulum, however, we find that it is possible to walk with exactly zero stance leg work even though the work done on the center-of-mass is finite; all the work is performed by the platform as the leg remains exactly constant length, with no push-off or heel-strike impulses. See Supplementary Video 1 for animations of these walking motions.

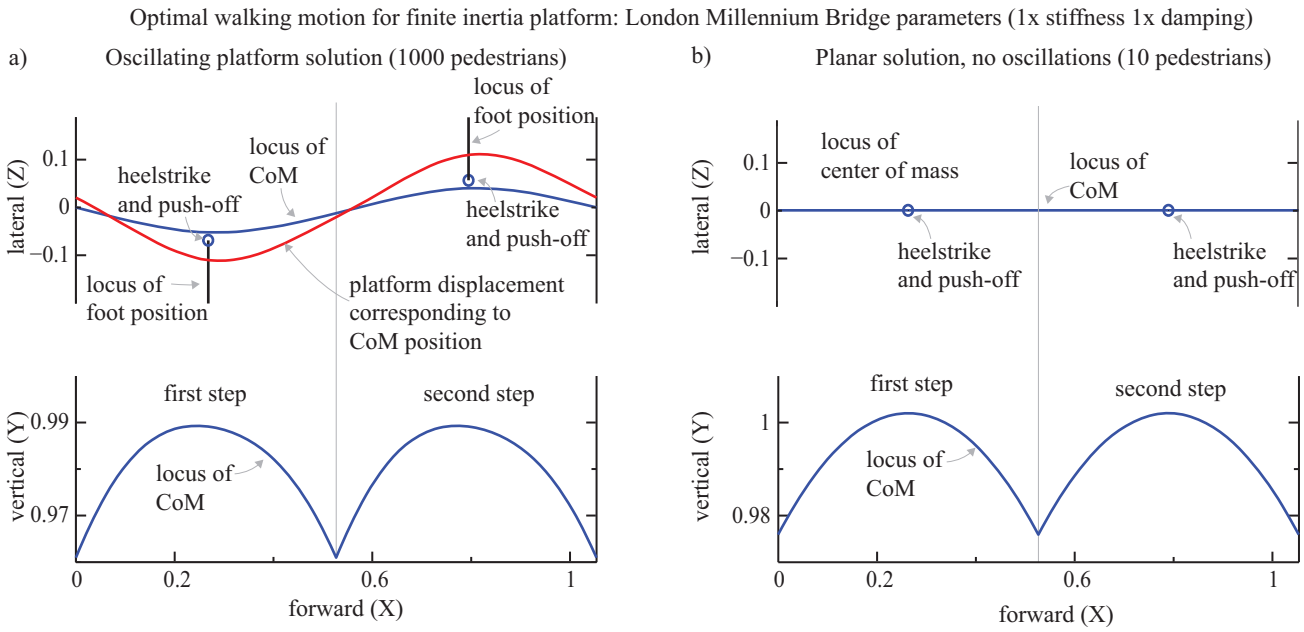

Figure S2: Optimal body motion for walking on finite inertia platform. The results correspond to London Millennium Bridge parameters (1x stiffness and 1x damping) for (a) $N_{\text{pedestrians}} = 1000$ pedestrians and (b) $N_{\text{pedestrians}} = 10$ pedestrians. The top and side view of the body trajectory is shown; also shown in the top view is the resulting bridge oscillation as a function of the body's forward position. Supplementary Video 2 shows 3D animations of these walking motions and figure 4 of the main manuscript shows the 3D walking trajectory corresponding to panel-a.

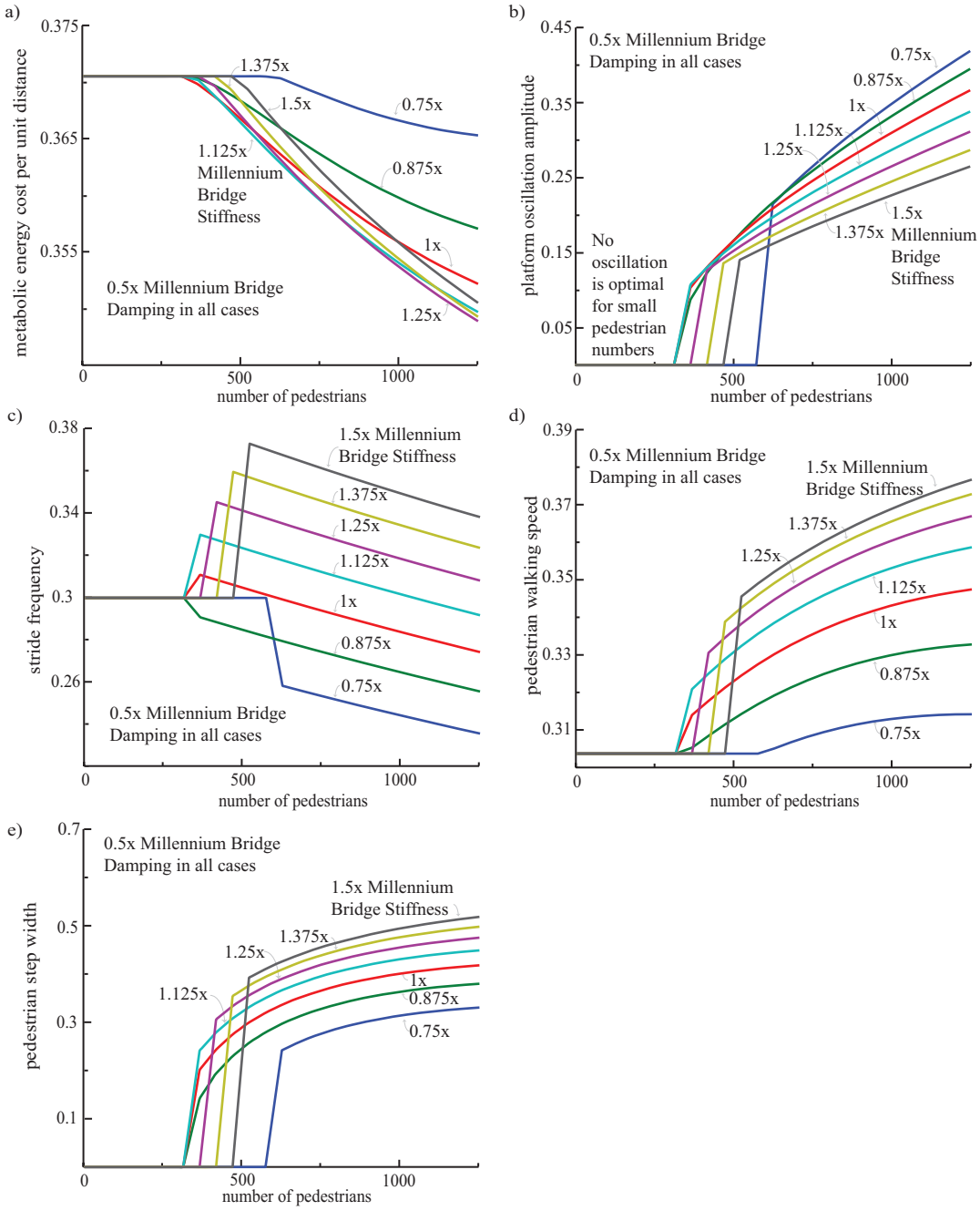

Figure S3: Optimal walking on the finite inertia platform at 0.5x Millennium Bridge damping for varying stiffness. The variation in a) metabolic energy cost per unit distance b) platform oscillation amplitude c) stride frequency d) pedestrian walking speed e) pedestrian step width show that non-oscillating solutions are optimal at low pedestrian numbers and oscillating platform solutions at higher pedestrian numbers. We see that the pedestrians choose to walk with larger step-width at a speed faster than their optimal on steady ground when the platform oscillates. This figure reproduces and extends panels a and b in figure 3 of the main manuscript.

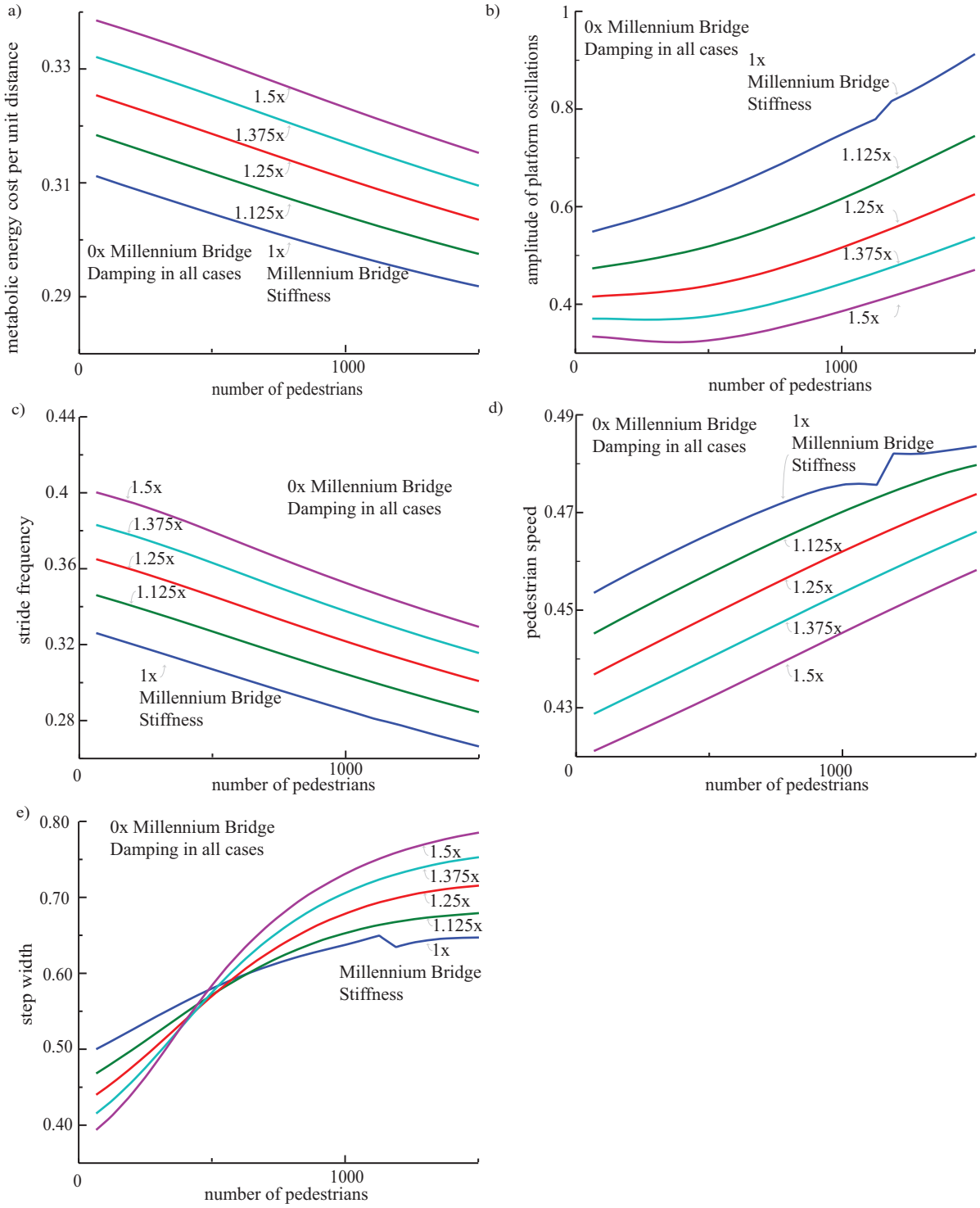

Figure S4: Optimal walking on the finite inertia platform at zero damping for varying stiffness. The variation in a) metabolic energy cost per unit distance b) platform oscilation amplitude c) stride frequency d) pedestrian walking speed e) pedestrian step width show how the pedestrian and the platforms' movement changes between the oscillating and non-oscillating platform solutions. The critical number of pedestrians for a shaky platform drops to essentially 1, as one finds oscillating platform solutions to be optimal for even one person. We no longer have the complicated pattern for varying stiffness that is seen in the 0.5x damping case (figure S3).

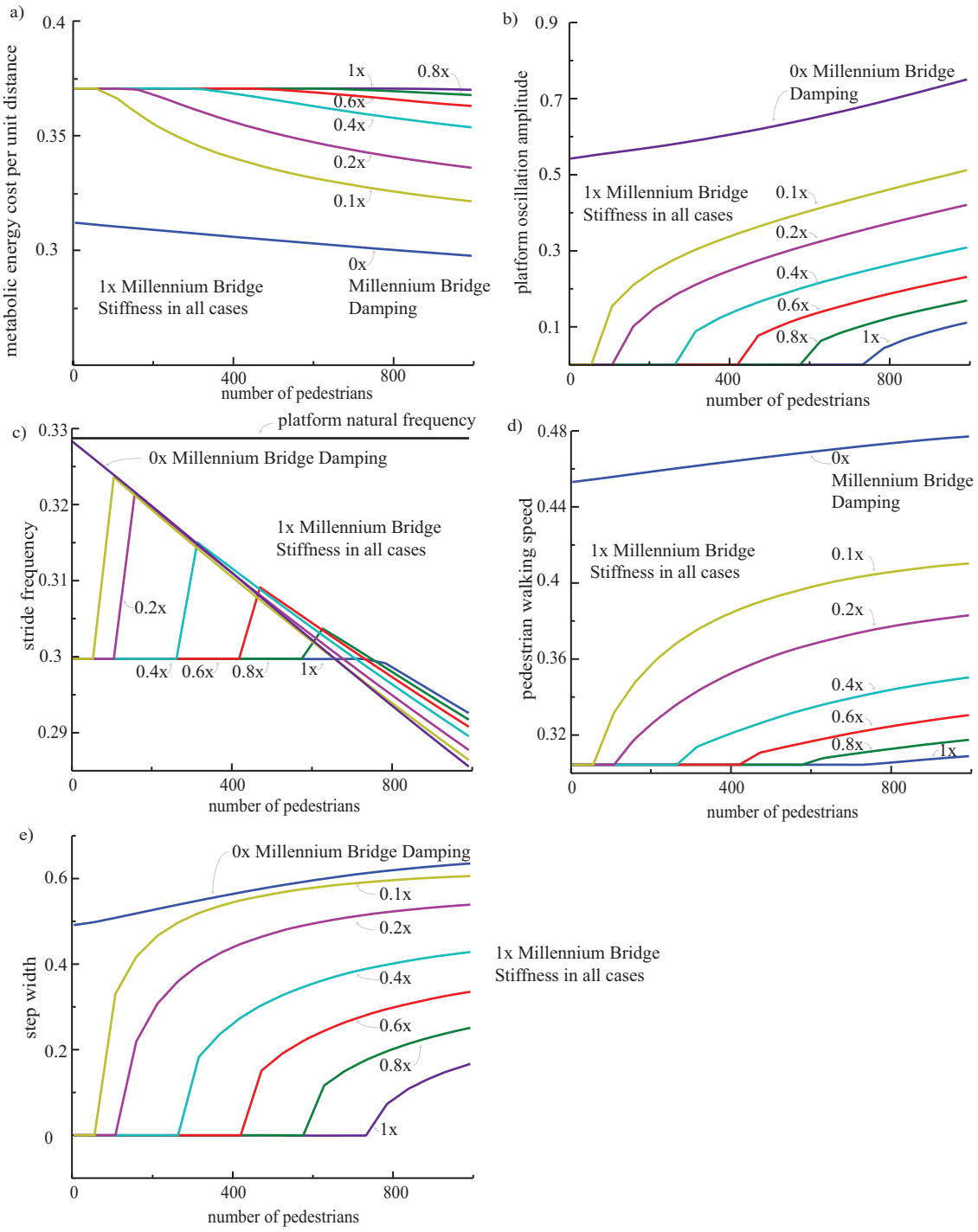

Figure S5: Optimal walking on the finite inertia platform at the exact Millennium Bridge stiffness for varying damping. The variation in a) metabolic energy cost per unit distance b) platform oscillation amplitude c) stride frequency d) pedestrian walking speed e) pedestrian step width show how the pedestrian and the platforms' movement changes between the oscillating and non-oscillating platform solutions. Increasing damping makes the oscillating solution less optimal; decreasing damping lowers the critical number of pedestrians needed for the oscillating solution to be optimal. This figure reproduces and extends panels c and d in figure 3 of the main manuscript.

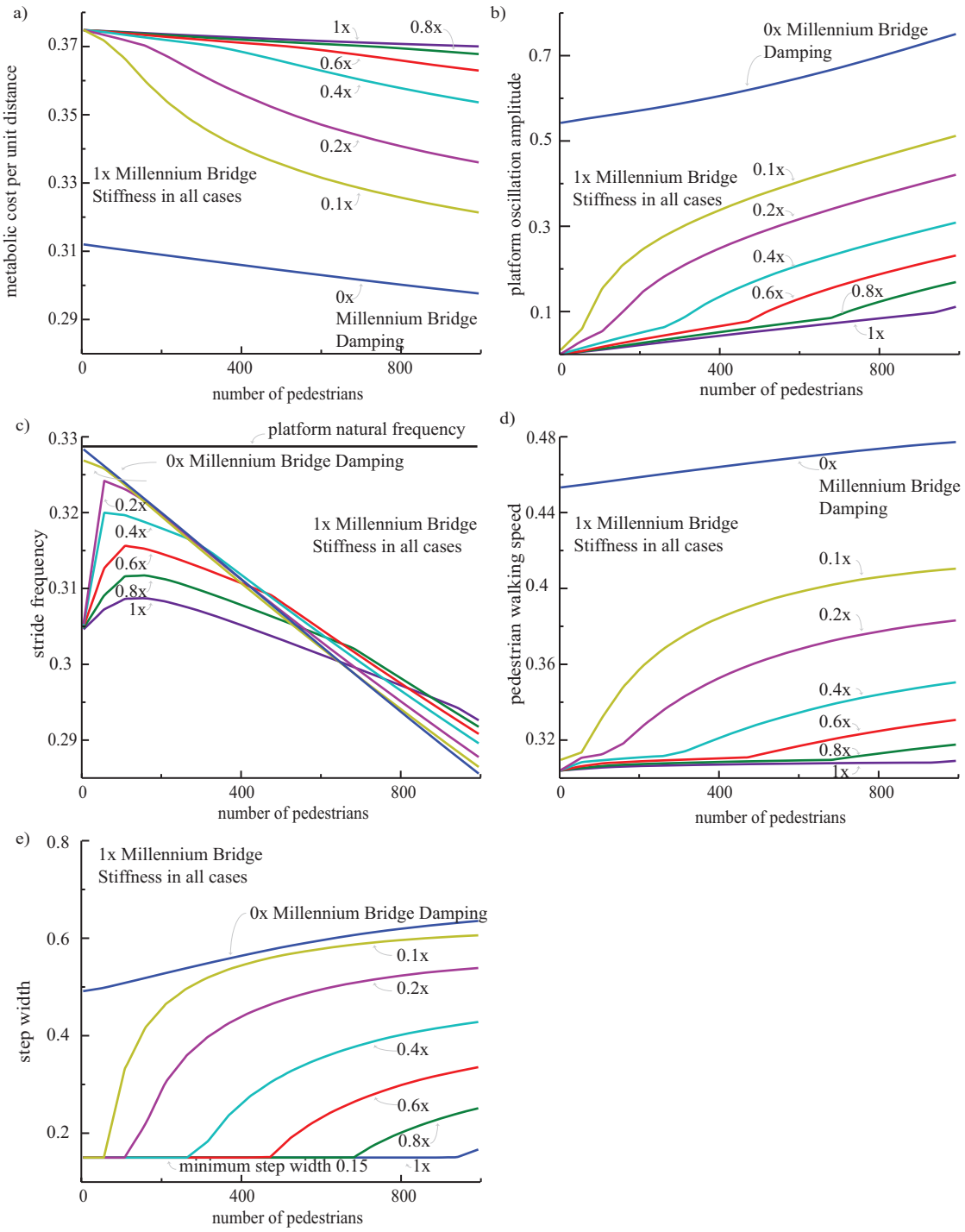

Figure S6: Optimal walking for the finite inertia platform at the exact Millennium Bridge stiffness for varying damping, but with a minimum step-width of 0.15 used to constrain the motion. The variation in a) metabolic energy cost per unit distance b) platform oscillation amplitude c) stride frequency d) pedestrian walking speed e) pedestrian step width show how the pedestrian and the platforms' movement changes between the oscillating and non-oscillating platform solutions. We see that the minimum step-width constraint leads to oscillations at lower number of pedestrians, but the metabolic cost of these oscillating solutions does not decrease below the corresponding cost for the non-oscillating solution. In essence, this figure is identical to the previous figure (figure S5) for large pedestrian numbers for which the optimal step width is greater than the minimum prescribed; for smaller pedestrian numbers, we obtain optimal solutions with the minimum possible step width.

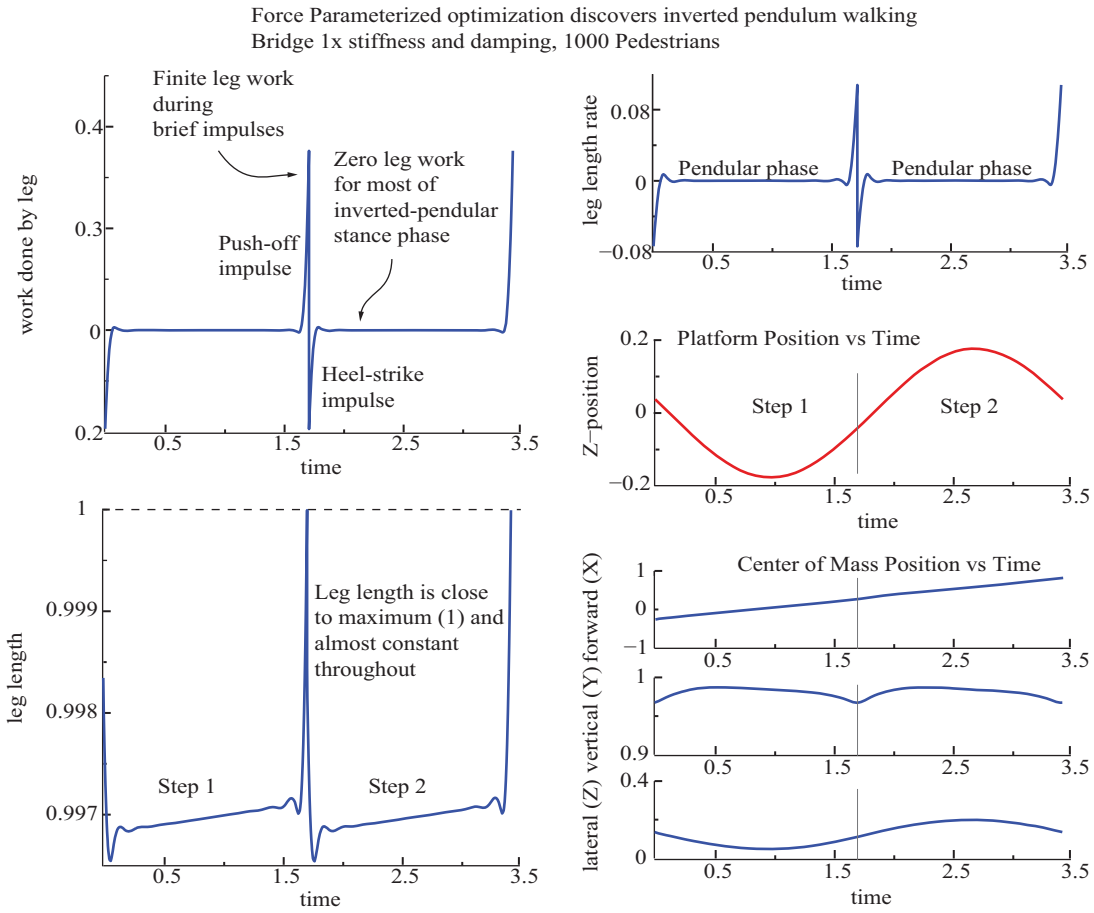

Figure S7: Force Parameterized optimisation discovers inverted pendulum walking on a shaky bridge. These are results from an optimisation calculation on a bridge with 1x stiffness and 1x damping with $N_{\text{pedestrians}} = 900$, without assuming that the motion is inverted pendulum. Instead, the leg forces were allowed to be piecewise linear functions of time with $N_{\text{segments}} = 18$ segments per step. The optimisation naturally discovers an inverted-pendulum-like gait, with the leg length mostly remaining near the maximum leg length and almost constant. More significantly, the leg work remains close to zero for most of stance phase and becomes non-zero only near the step to step transitions, with push-off and/or heel-strike impulses. Similarly, the leg-length rate remains close to zero for most of the stance phase and becomes substantially higher during the push-off and heel-strike impulses.

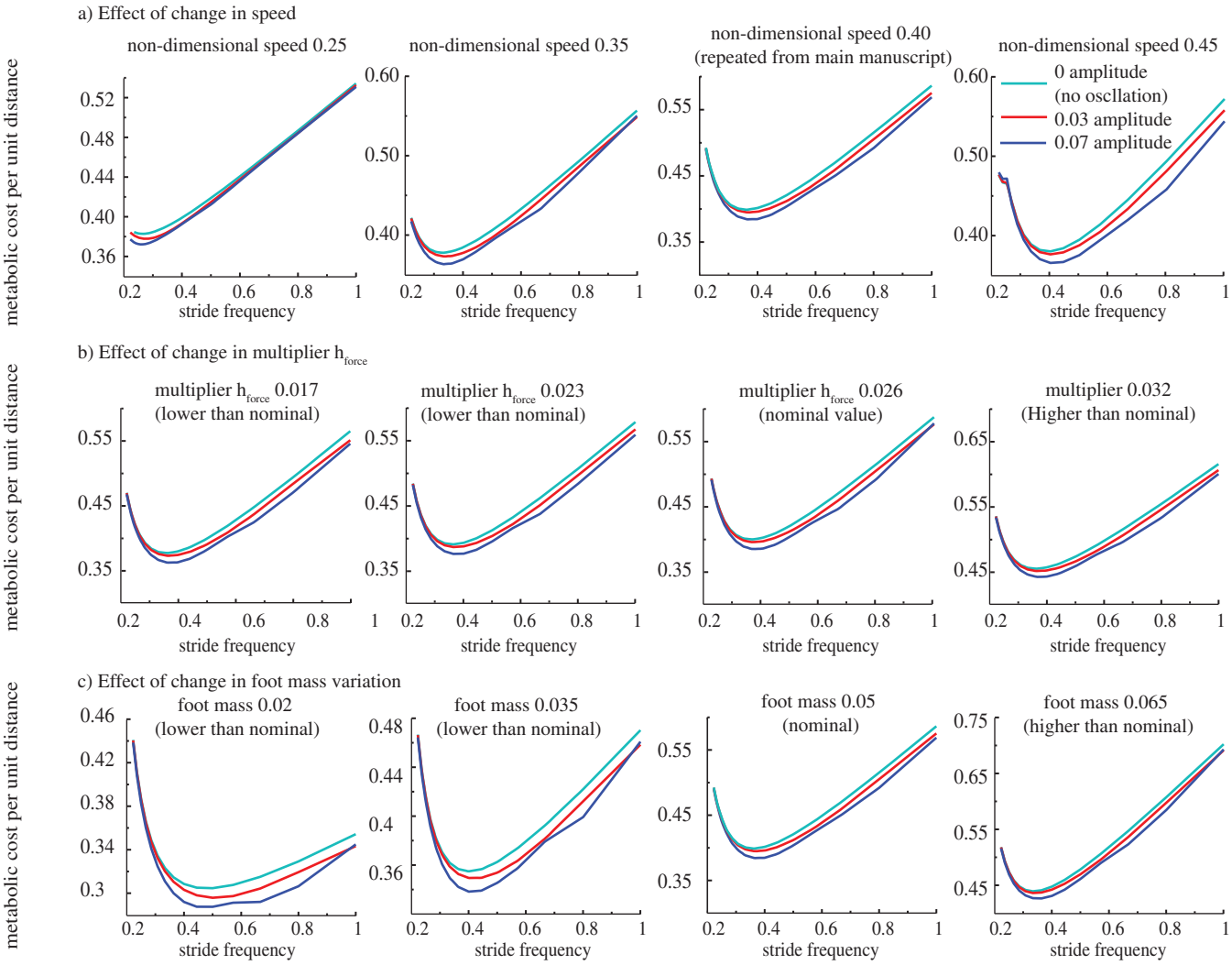

Figure S8: Energy reduction persists for a range of model parameters: shaken treadmill. These figures show that the energy reduction for walking on an oscillated infinite inertia treadmill persists for changes in walking speed, force multiplier η_{force} and foot mass. a) Increasing the selected walking speed increases the corresponding optimal stride frequency for the model. b) Increasing the force multiplier η_{force} does not change the optimal body motion at any stride frequency, and thus only moves the cost curves up. c) Increasing foot mass increases the energy cost at higher stride frequencies but does not affect lower stride frequencies to the same degree, the optimal stride frequency does not change.

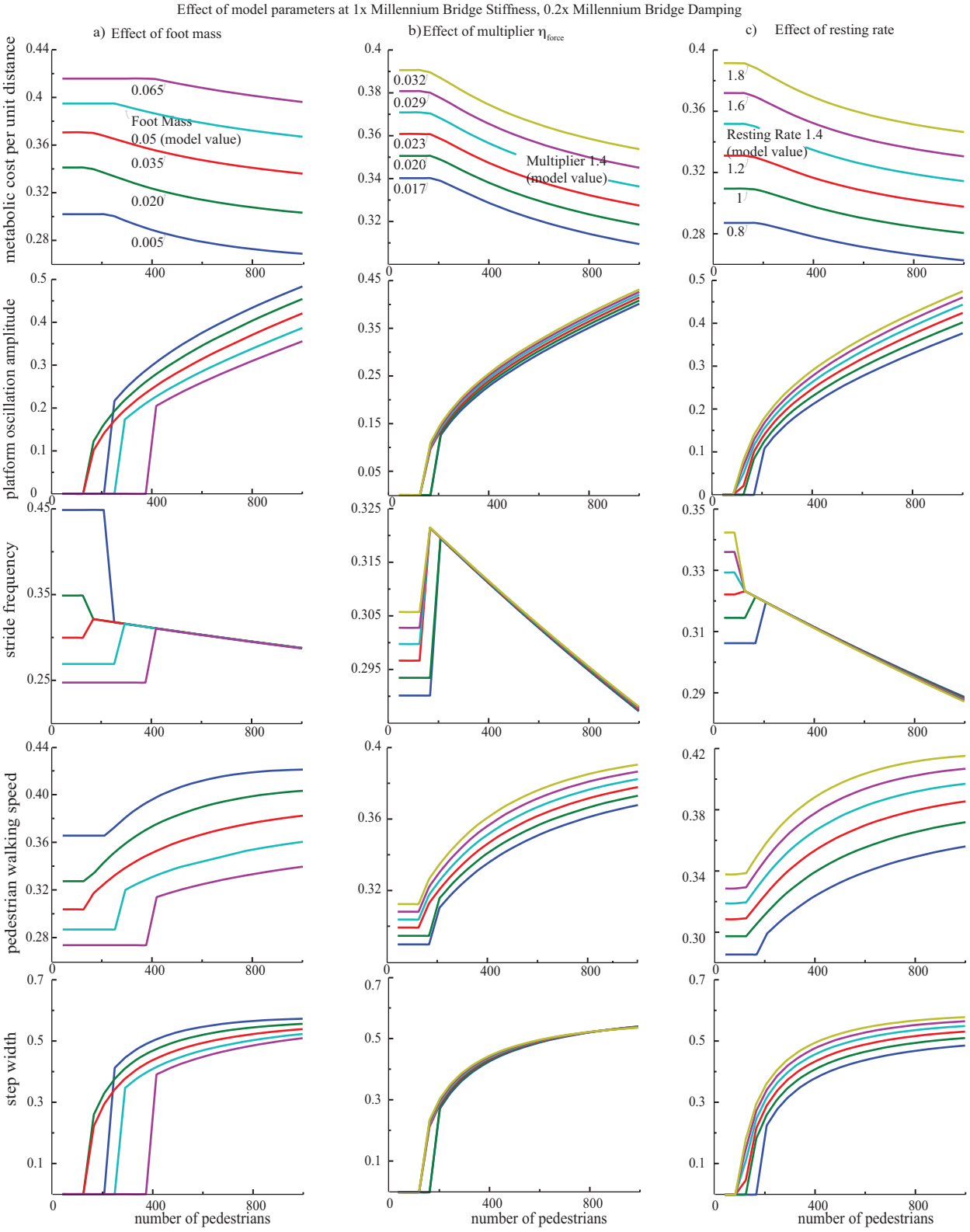

Figure S9: Energy reduction persists for a range of model parameters: shaky bridge. These figures show that the energy reduction for walking on a finite inertia bridge persists for changes in a) foot mass, b) force multiplier η_{force}, and c) resting rate. Also, shown are variating in platform amplitude, stride frequency, walking speed, and step width for a range of pedestrian counts, for different values of each of these parameters. We use 1x Millennium Bridge stiffness and 0.2x damping for all these calculations.

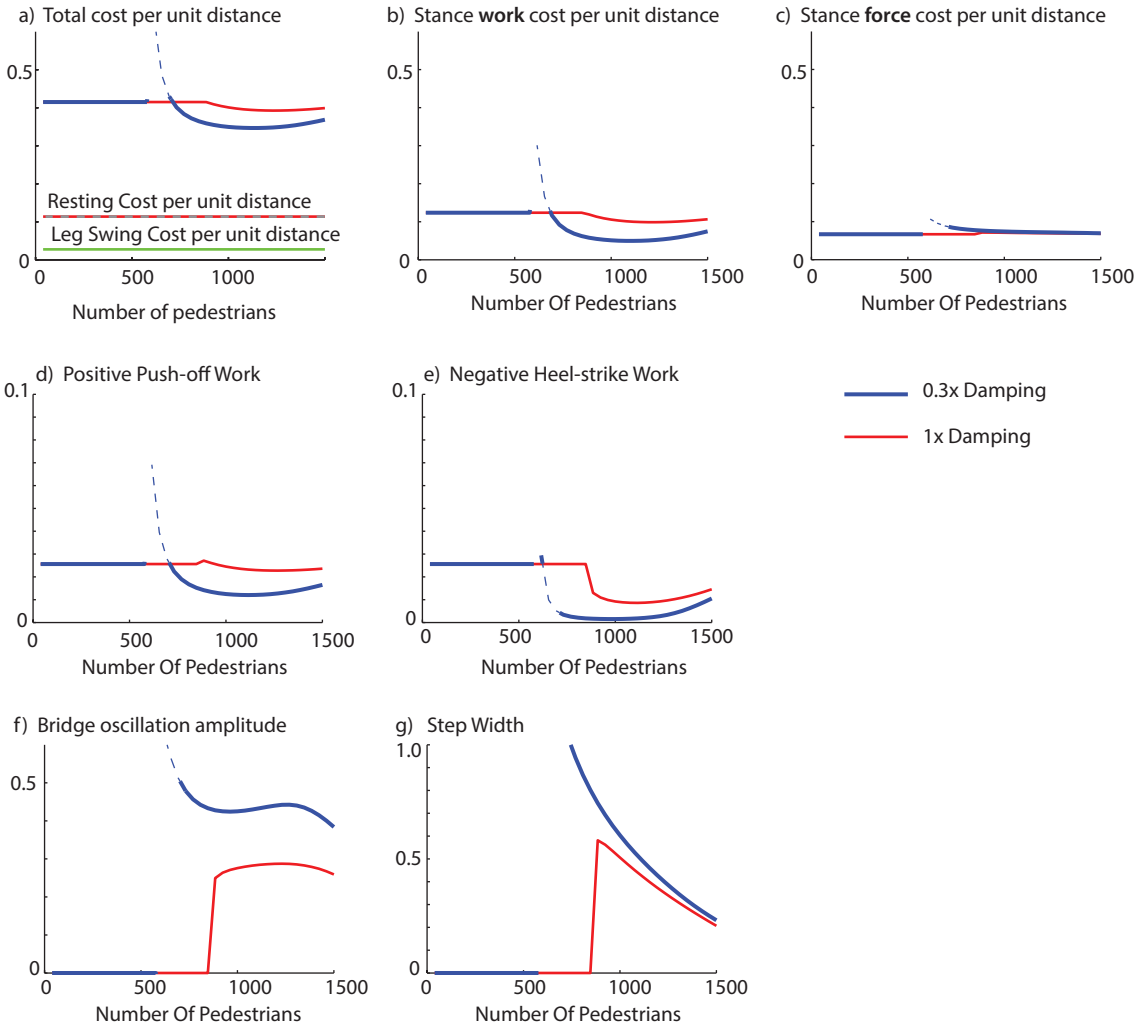

Figure S10: Cost components on a shaky bridge, planar versus non-planar solutions, fixed speed and stride length. We consider a shaky bridge with 1x stiffness and two different damping values (0.3x and 1x). We fix the forward speed at 0.4 and forward stride length at 1.4 (stride frequency 0.286). For low pedestrian numbers, all the quantities plotted are constant, because the optimal motion is planar inverted pendulum and all cost terms are constrained by speed and stride length. Further, independent of pedestrian number, the swing cost and resting cost are fixed. When the pedestrian number increases beyond the shaking threshold, the total cost decreases: all of this reduction is due to the stance work cost (b), which is enabled by a reduction in the positive stance work during push-off (d) and an even greater reduction in the negative work during heel-strike (e). Near the threshold, a shaking solution has a higher leg force integral cost than a planar solution, but this increase is much smaller than reduction in the stance work cost.

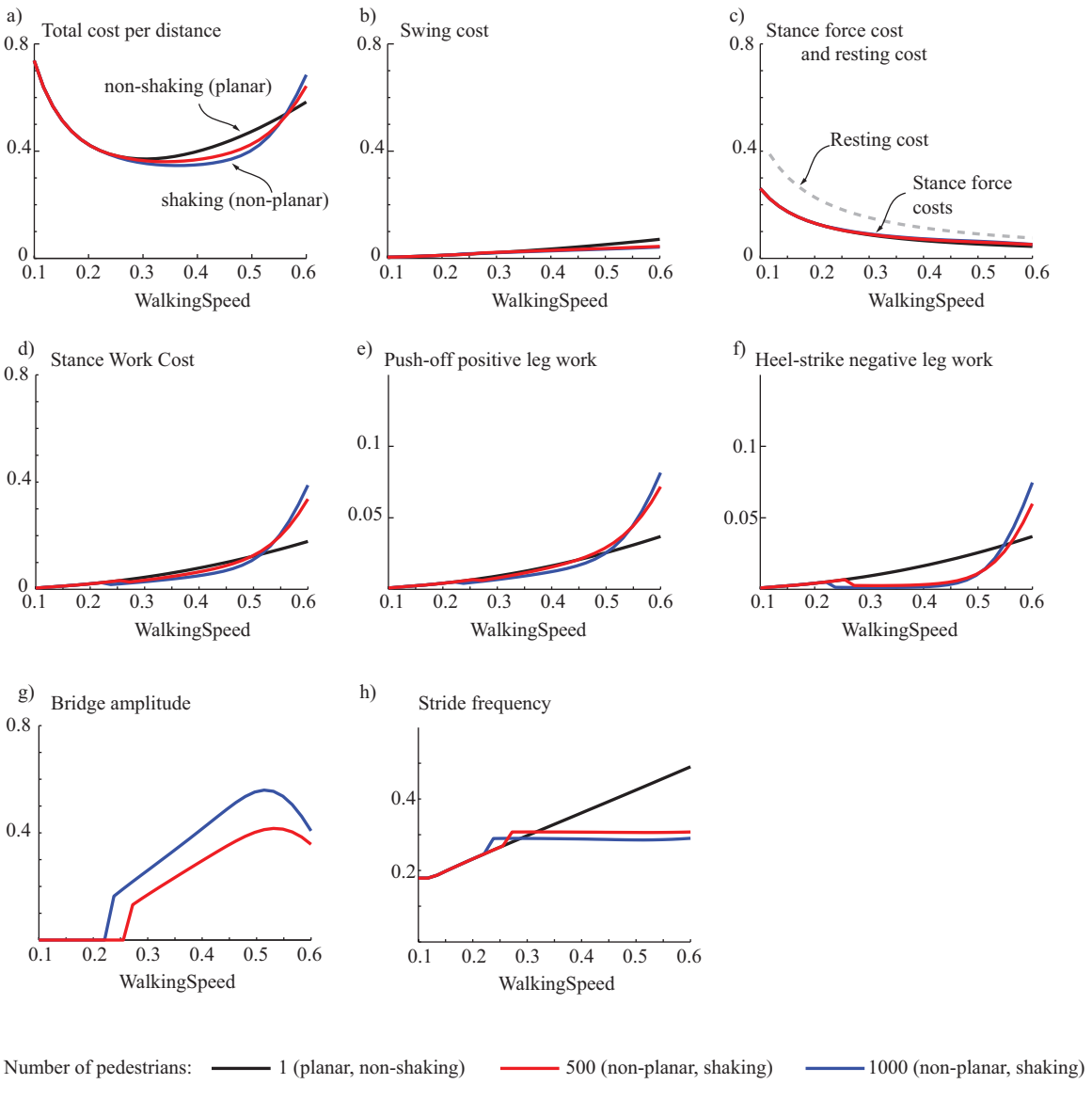

Figure S11: Cost components on a shaky bridge, planar versus non-planar solutions. Here, we consider a shaky bridge with 1x stiffness and 0.3x damping. We determine optimal solutions as a function of speed for three different numbers of pedestrians: $N_{\text{pedestrians}} = 1$, which corresponds to a planar non-shaking solution, $N_{\text{pedestrians}} = 500$ (red) and $N_{\text{pedestrians}} = 1000$ (blue), which correspond to non-planar shaking solutions.

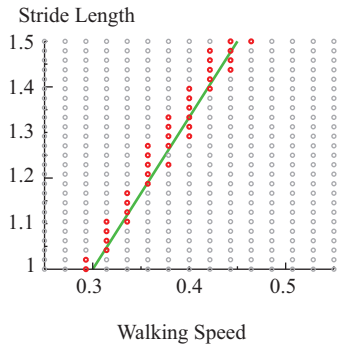

Figure S12: When is shaking a shaky bridge better than non-shaking planar walking. We found the optimal solution for $N_{\text{pedestrians}} = 1000$ for a range of speeds and step lengths (equivalently, stride frequencies). We found that only for a small range of speeds and stride lengths is a shaking solution better than a non-shaking planar solution, shown by red circles. The green line is the line corresponding to a stride frequency of 0.3 (that is, stride length = 0.3 speed). Thus, we see that the regime where shaking is better corresponds to a nearly constant stride frequency that is close to the bridge's natural frequency. The results correspond to 1x stiffness, 0.3 damping.

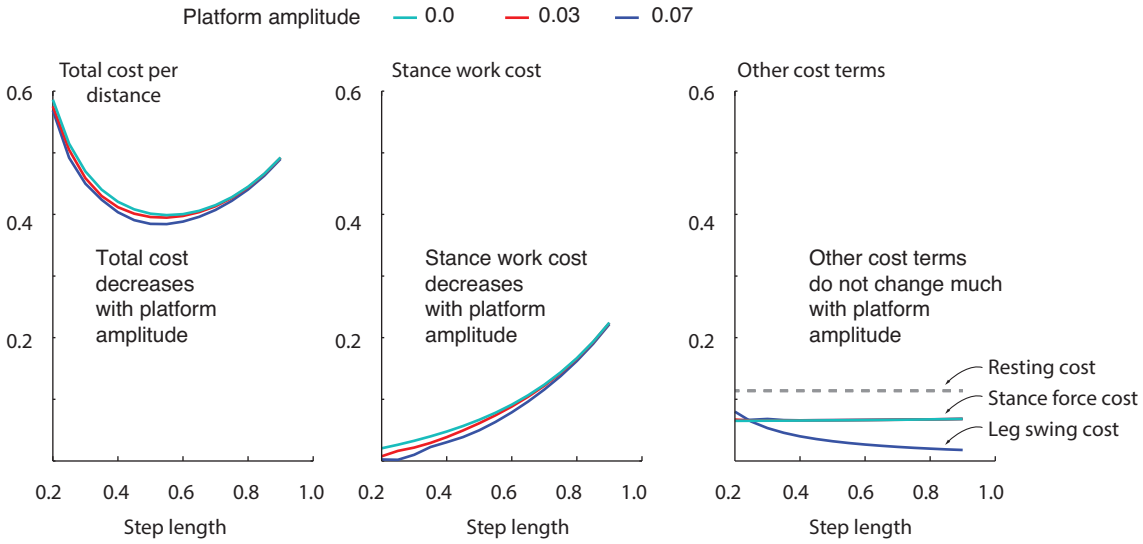

Figure S13: Cost components for the shaken treadmill. Components of the energy cost per unit distance for non-dimensional speed 0.4 (1.2 m/s), at three different platform oscillation amplitudes. Notice that the most of the reduction in total cost is due to the reduction in the reduction in the stance work cost. The resting cost and swing cost do not change with platform amplitude. The stance force cost does increase with increased platform amplitude as the legs become more tilted with the vertical, but this increase is much smaller than the decrease in stance work cost. The stance work cost reduction comes from an equal reduction of both positive and negative leg work, which are equal to each other in the shaken treadmill case.